BIROn - Birkbeck Institutional Research Online

Brown, Jason and Roberts, Gerald P. (2023) Repeated, cross-cutting and spatially migrating outflow channel formation, Grjótá Valles, Mars. Journal of Geophysical Research: Planets , ISSN 2169-9097.

Downloaded from: https://eprints.bbk.ac.uk/id/eprint/50563/

Usage Guidelines:
Please refer to usage guidelines at https://eprints.bbk.ac.uk/policies.html or alternatively contact lib-eprints@bbk.ac.uk.

Repeated, cross-cutting and spatially migrating outflow channel formation, Grjótá Valles, Mars

Jason R. Brown, Gerald P. Roberts,
Department of Earth and Planetary Sciences, Birkbeck, University of London, WC1E 7HX, United Kingdom

Abstract: Cross-cutting relationships and the incision history for multiple outflow channels have been mapped and studied to establish their relative chronology in Grjótá Valles, Mars, in order to establish whether observed geomorphic channels were formed in a single event or multiple events. The relative chronology can be established by mapping cross-cutting relationships between channel margins and successive incision, where later channels incise downwards into older channels. We show that the source areas of five distinct channels can be established, with younger channels progressively sourced further to the east along the Grjótá Valles fault system, and incising downwards into older channels. The channels resemble examples interpreted elsewhere as cut by catastrophic aqueous flow processes (diluvial) due to their regional morphology, the presence of streamlined islands surrounded by anabranching channels marked by incision, recessional terraces and longitudinal erosional grooves, however turbulent lava flows may also have been involved. That five distinct flows occur progressively further to the east may indicate the progressive propagation from west to east of the processes at depth that released the fluid responsible for cutting the channels, such as dike propagation and associated seismicity. Our observation of multiple flows and channel formation episodes implies instantaneous volumes of fluid that are smaller than that for a single flow interpretation.

Plain Language Summary:

Channels attributed to catastrophic aqueous flows have been suggested to exist on Mars, but debate surrounds the relative roles of water versus lavas in forming the channel morphologies, and the large volumes of fluid required to form the channels if they formed during single events. Our study of a channel system associated with Grjótá Valles, where channels emerge in the vicinity of faults, fissures and fractures, demonstrates cross-cutting relationships between channels that can be mapped back to five distinct channel sources. This suggests at least five separate channel forming events. The channels show geomorphic features that resemble those formed by catastrophic aqueous flows on the Earth, and lack features suggesting the filling of channels by lavas, but we cannot rule out that turbulent lava flows may also have helped to cut the channels. We use these observations to discuss the processes that led to formation of the channels for this portion of Mars.

Introduction

Three large channel systems exist around Cerberus Planitia, Mars (Athabasca Valles, Marte Valles, Grjótá Valles; Burr et al. 2002), but uncertainty exists with regard to whether the channels formed during single events of multiple events, with the former leading to concerns about the very large volumes of fluid required. In this paper we describe new observations of cross-cutting relationships between channels in Grjótá Valles that imply at least five separate channel forming events. We show that the cross-cutting channels can be mapped upstream to five separate channel sources along the present trace of a system of faults, fractures and fissures in Grjótá Valles that form part of Cerberus Fossae. Cross-cutting relationships show that the fault, fracture and fissure system formed after the channels. Our observations of the channels show landforms that resemble those produced by aqueous flows on the Earth, but the flow of turbulent lava flows may also have played a role in their formation. Other nearby channel systems (e.g. Athabasca Valles) have been shown to exhibit clear signs of lava infills to their pre-existing channels (e.g. Jaeger et al. 2007; Jaeger et al. 2010). We report our observations derived from detailed mapping, topographic profiling, and identification of cross-cutting relationships, and use this to discuss whether the channels were cut by a single event or multiple events and what processes formed these channels.

It is unclear if these channels formed during single or repeated flow events (Burr et al. 2002), and this therefore introduces uncertainty with regard to estimated flow volumes and discharge rates. As to what process formed the channels, three hypotheses (aqueous, lava, mudflow) have been considered and we look at each in turn.

The hypothesis that the channels in Grjótá Valles result from aqueous flows has existed for some time (Barker and Milton, 1974, Burr et al., 2002, Head et al., 2003, Morgan et al., 2013, Plescia, 2003). The cause of the channels formation has been interpreted as either the result of magma-induced melting of the cryosphere (Berman and Hartmann, 2002; Burr et al.,2002; Head et al., 2003), outflow of water from a breached aquifer above an intruding dike beneath the fossae (Carr, 1979; Burr et al., 2002; Plescia, 2003), release of water from a sub-cryosphere aquifer a few kilometres thick, and tens of kilometres in lateral extent (Manga, 2004), or from another subsurface origin (Jones at al., 2011). A number of researchers have suggested that large mega floods occurred (Kattenhorn and Meyer, 2010; Burr et al., 2002, 2009) across parts of the Cerberus Fossae, flowing through the three Amazonian aged flood channels within the region (Grjótá Valles, Marte Valles, and Athabasca Valles), with the emanation points of these floods not conclusively identified, although generally thought to be the fossae themselves (Burr et. al 2002, 2009). It has been suggested that the flows that formed such channels were very large, with very high discharge rates (e.g. 1-8 x 10^6 m^3 s^{-1} for the nearby Athabasca Valles channel system; Keszthelyi et al. 2007), because, for example, the Grjótá Valles channels cover a region of ~90,000 km^2. An alternate hypothesis is that the flow of turbulent lavas was a possible mechanism for cutting channels (Jaeger et al. 2010). This uncertainty gives rise to a number of questions including how could the implied large volumes of water/lava needed for such flows be released, and where could such volumes of water be stored. It has been suggested that the fault system running through Grjótá Valles, that forms part of Cerberus Fossae, is formed due to dike emplacement and this facilitated flow formation (e.g. Head et al., 2003). Numerical modelling has been used to link dike-related heat flow and flow volume on Mars in general, and shows that such dikes would in some cases be able to produce heat to melt ground ice which could produce flow water to create channels and/or landforms similar to those described herein (e.g. McKenzie and Nimmo, 1999, Wilson and Head 2002, Plescia 2003). Head et al. (2003) suggest for Athabasca Valles, which like the Grjótá Valles emanates from Cerberus Fossae, that dike emplacement produces surface cracking, localised volcanic eruptions, cryospheric cracking, and release of pressurised groundwater from beneath the cryosphere. However, Head et al. (2003) note that the required aquifer permeability is larger than commonly encountered on Earth, meaning that either water is transported through the subsurface by a highly efficient, as yet unknown mechanism, and/or the volume flux values are overestimated. Furthermore, the existence of voluminous sub-surface ice is debateable. Observations of seismic wave velocity of the Martian crust suggest that the subsurface is not ice-saturated (Manga and Wright, 2021); however, their findings do not rule out the possibility of the existence of groundwater. However, support exists for sub-surface igneous heat sources (i.e., dikes along Cerberus Fossae) as lavas have been identified in some locations infilling the channels emanating from it (e.g. Keszthelyi et al. 2000, Burr et al. 2002, Plescia 2003, Jaeger et al. 2007, Jaeger et al. 2010). Volcanic centres have been mapped (Plescia 2003), and observations suggest possible dikes exposed on the floor of Cerberus Fossae (Head et al. 2003). Observations supporting the existence of lava infilling channels include (a) the presence of so-called ring-mound landforms imaged with HiRISE (High Resolution Imaging Science Experiment), which have been interpreted as volcanic (rootless) cones formed as lavas heated underlying groundwater causing steam explosions (Jaeger et al. 2007), (b) the presence of thin, concentric, lobate flow fronts that indicate overlapping lavas (Jaeger et al. 2007), and (c) the presence of platy-flow or platy-ridged surfaces indicating lava crusts (Chapman et al. 2010, Keszthelyi et al. 2000). However, the links between aqueous and lava processes, if they exist, remain elusive partly due to the uncertainty with regard to flow-rates and durations of flow, which are ultimately connected to whether multiple or single flow episodes produced the channels.

An alternate hypothesis is that lavas formed the Grjótá Valles, with the action of lavas as the dominant process in channel formation (Leverington, 2004, 2006, 2011, 2018). This hypothesis was supported by observations of geomorphic/geologic features on the Moon and Venus. These features are similar to those reported from channels on Mars, such as sinuous channels, inner channels, anastomosing reaches, streamlined erosional residuals, branching channel patterns, and reaches suggestive of lateral or vertical erosion (Leverington 2011). Furthermore, the formation of channels by lavas does not rely on the very large hydrological flow rates, sub-surface permeabilities, hydrologic head considerations, implied water abundances implied by an aqueous model, that do not concur with geochemical and mineralogical observations, and the lack of terrestrial analogues (Leverington 2011). However, it is implied that if lavas did dominate channel formation, lava morphologies should be identifiable, such as lobate flow fronts, upstanding flows, platy-ridges, knobs, break-outs or rootless cones that characterise lava-infilled channels described nearby on Mars, such as for Athabasca Valles, and they do not resemble sinuous rilles that are commonly associated with lava processes (Jaeger et al. 2007).

A third possibility is that channels formed during the passage of mudflows. Studies by Brož at al. (2020) looking at how the instability of water within a mud flow changes the mud behaviour showed that mud exposed to an atmospheric pressure and temperatures as low as that on Mars could propagate in a similar way to some terrestrial lava flows, notably pahoehoe flows. They showed that experimental mud flows in a low pressure/temperature chamber propagate like terrestrial pahoehoe lava flows, with liquid mud spilling from ruptures, then refreezing to form a new flow lobe. The channels would exhibit features characteristic of such mud flows, such as upstanding rubbly chaotic mudflow deposits with lobate fronts, or distributary aprons.

We made detailed observations of the geometries, cross-sectional profiles, and cross-cutting relationships for geomorphic features. We also mapped the landforms to investigate whether the channels formed in single or repeated events. We mapped the geomorphology of the channel system and fractures using Context Camera (CTX) and HiRISE images from the Mars Reconnaissance Orbiter (MRO), measured cross-sectional profiles of landforms using Mars Orbiter Laser Altimeter (MOLA) data, and assessed the timeline of events. Our interpretation is that at least five distinct channel forming events occurred in Grjótá Valles. The channels are dominated by landforms cut by high rates of water/turbulent-lava flow, with these flows pre-dating development of vertical offsets across the faults and fractures that are present. We consider this as evidence of at least five asynchronous fluvial flow episodes that occurred in this region of Mars.

Background

The Grjótá Valles outflow channel system emanates from the northernmost Cerberus Fossae (Figure 1 a. and b.). The fault system of the northernmost Cerberus Fossae is a ~200 km long set of *en echelon* fissure segments located between

16.175°N / 160.563°E, and 15.202°N / 163.666°E (Brown and Roberts, 2019). The WNW-ESE orientation of the fissures would indicate that the fractures are sub-radial to Elysium Mons (Fig. 1).

The faults in this region (Fig. 1 b.) are relatively recent in that they crosscut pre-existing features of known, relatively young age with the fossae also offsetting late Amazonian Cerberus lavas and older inliers (Tanaka et al., 2005). Using crater counting methods the ages of the youngest lavas offset on the nearby Cerberus Fossae are <10 Ma (Hartmann & Berman, 2000; Head et al., 2003; Vaucher et al., 2009), which would imply that the fossae are even younger. However, studies by Golder et al., (2020) show that discrepancies in the ages of craters could be due to rheological changes produced during lava emplacement, meaning that at locations proximal to the inferred source of the lava, larger craters yield older model ages due to the weaker, more porous rock. At more distal locations from the inferred source of the lava, smaller craters yield younger model ages due to stronger, non-porous rock. Within the extent of the Grjótá Valles flow tract (Fig 1. b.) crater counting suggests that the implied ages range from 55 Ma (proximal) to 33 Ma (distal) (see Figure 2 for locations of crater counts) (Golder et al. 2020). Although uncertainty exists regarding how to interpret these ages, the fact that faults cross-cut and offset the surface would confirm the relatively young age of the faulting. The lavas in Grjótá Valles have been interpreted as lava emplaced as single flow units due to their morphologies and mapped extents (Jaeger et al., 2010; Hamilton, 2013).

Burr et al. (2002) note that the Cerberus Plains show three spatially and temporally distinct, young aqueous flow channel systems (Fig. 1 a. & b.). One of these flow channel systems that we study herein, the unnamed northern channel system, has been suggested to be a ~100 km wide channel for water emanating from the northernmost Cerberus Fossae. It extends for a few hundred kilometres from the northernmost Cerberus Fossae to the north-east, then heading south-east before its surface expression becomes indistinct. Burr et al. (2003) described fluvial geomorphic features indicating that water emanated from the source area of the northernmost Cerberus Fossae, flowed eastward, and then flowed south-east. Our study draws upon the work of previous studies such as Burr et al. (2002) who suggested that repeated flow events may be responsible for the channels, and Burr et al. (2002) and

Plescia (2003) who suggested that the area exhibits the typical characteristics of channels produced by the catastrophic release of water, such as a well-defined source area, low sinuosity channels, and longitudinal grooving of channel floor, but this is a source of debate as described above (Leverington 2011). Due to the resolution of data available to them at the time, they were unable to demonstrate cross-cutting relationships between individual channel sections or provide detailed observations of the source of flows.

Method

We used the CTX image mosaic for Mars, a mosaic composite of all the Mars Reconnaissance Orbiter (MRO) Context Camera (CTX) images available (~6 m per pixel) and HiRISE images (~30 cm per pixel) from two instruments on the MRO to study an area of ~70,000 km^2 (Fig. 2). We mapped the geomorphology of the channel system and fractures, using a combination of CTX and HiRISE images, constrained the cross-sectional profiles of landforms using MOLA point data, and combined these observations to gain a chronology of the processes involved. We used Google Earth (which uses spherical normal (equatorial) variant of the Mercator projection for its maps) and HiView (which uses equirectangular projection map projections) to study and analyse the images.

Initial observations highlighted the presence of cross-cutting channels in several locations. Initially, we concentrated on mapping these locations and also attempted to map these back to sources where channels emanated from Cerberus Fossae (Figure 3). Mapping the channels back to their sources was found to be very important in delineating the total number of channels that could be identified, because some cross-cutting relationships may be between distributary channels where the initial channel separates into a multiple courses downstream. We were careful to make sure this did not lead to an exaggeration of the number of separate channels because the five examples we have identified can all be mapped back to a separate sources without interruption by a cross-cutting channel (Figure 12). Identification of cross-cutting relationships that can be mapped back to the channel sources was possible for some locations (Figures 4 through to 10), but for others we were unable to map back to the sources due to ambiguous relationships on the imagery, and we include these as Supplementary Figures S1 through to S4. In other words, Supplementary Locations (A through D) (Fig. 2 & Figs. S1 through S4) were constructed in an identical manner to Locations (1 through 7) (Fig. 2 & Figs. 4 through 10) except that their purpose was to assist in delineating the possible boundaries between two different flow areas in the downstream region, and thereby helped us develop our regional map (Fig. 2).

Once the areas exhibiting cross-cutting relationships were identified, we then used MOLA Precision Experiment Data Records (PEDRs) to produce transects across the location areas. We did this to measure channel depths and hence amounts of channel incision. The laser spots cover an area of ~160 m diameter, spaced every ~300 m, and this introduces uncertainty in the elevation values estimated to be 1-10 m (Albee et al. 2001). Thus, we only report observations based on MOLA data if the vertical differences were >10 m. We were also careful not to use laser returns from locations where the elevation changes dramatically at < 160 m horizontal length-scale, excluding such locations by examining shadow lengths on CTX and HiRISE images. For individual locations we found that MOLA data were available from about five to six transects for each location studied, and we used all available data points. From these data we constructed topographic profiles (distance / elevation) across each of the areas of interest (11 locations). These topographic profiles were then studied in conjunction with the location images and our mapping to assess cross-cutting relationships between different channels by determining whether younger features incised down into and hence post-dated older features, as well as to measure the depth of such channels, and to gain elevation information for geomorphic features. We also studied the illumination of images as these helped us understand the aspects of slopes.

We then colour coded geomorphic features separated by cross-cutting relationships to indicate a chronology for the geomorphic evolution. We then mapped between locations to produce a regional map of the channels, faults and their chronology (Figure 2). Once the location maps and topographic profiles were completed, and the regional map constructed, we then began to add flow lines to all maps, based upon the position and orientation of the different channels and the orientation of any geomorphic markers (such as depressions, linear features on the depression floor, linear features on the slopes of the depression margins, linear features on streamlined hills, and 'tear-drop' shaped hills) within the channels.

We then constructed topographic profiles along channels from MOLA data. These profiles were used to assess whether individual channels flowed downhill, a key criterion in any interpretation.

Results

We created geomorphic maps of seven locations. We start by describing how we differentiate and identify key geomorphic features that are widespread across the region, using Location 1 as a type location (Figure 4). For each feature, we initially describe it before interpreting its significance. Following this, we use these type examples to interpret features in Locations 2 through to 7 (Figures 5 through to 10; Supplementary Figures S1 through to S4).

Location 1 (Fig. 4)

Location 1 is centred at 15.70° N, 161.61°E, in the western portion of the overall channel system (Figure 2). It lies ~10 km south of the main system of faults, fractures and fissures that form part of Cerberus Fossae, but is crossed by smaller fractures that trend WNW-ESE. The area is a relatively flat plain with relatively low crater densities and several areas of higher topography with relatively high crater densities (see topographic profiles). The area also contains features that resemble channels and a streamlined island, and below we describe the five main features of note.

Descriptions of five geomorphic landforms at Location 1:

i) Depressions
Our observations suggest the presence of depressions that are visible on the CTX images, and are apparent in the MOLA profiles that cross their traces. The main depression runs NW-SE, is 3-4 km wide (Figs. 4 a, 4 b and 4 c) and is in the order of

35-40 m deep; it is crossed by profiles c’- c, d’- d, e’- e and f’- f (Figs. 4 a, 4 b and 4 c and topographic profiles c’- c, d’- d, e’- e and f’- f). Other depressions are shallower (< ~10 m) and in places run W-E, such as the examples that are crossed by the northern end of profiles a’- a and b’- b, and the southern end of profile c’- c. The depressions are visible due to illumination from the SW that produces shadows on the NE of features that slope towards the NE and brighter areas on features that slope towards the SW.

ii) Linear features on depression floor

These are 3-4 km long, ~50-100 m wide, defined by what appears to be a set of relatively smooth ridges, because they have shadows on their E or NE sides and relatively brightly illuminated W or SW sides (Fig 4 c). These ridges die out in both the NNW and SSE direction, terminating in places with lenticular-shaped ends.

iii) Linear features on the slopes of the depression margins

Linear features also exist on the slopes forming the margins of the depressions. We identify up to 9 sub-parallel examples in Figure 4 c, but note that they have embayed traces, that are in places sinuous and discontinuous. They differ from the linear features that exist on the depression floors because MOLA data show they exist on the depression margin slopes and hence they have shadows on one side (the NE side in Fig. 4c), but no relatively brightly illuminated opposite side. This implies that they resemble a set of steps cut into the slope on the margin of the depressions. MOLA data reveal that in places up to 9-10 of these linear features exist on slopes that are ~1 km across with relief of ~35-40 m, revealing that the individual steps are no more than a few metres high (e.g. Fig. 4 c and topographic profiles c’- c, d’- d, e’- e and f’- f).

iv) Linear features on streamlined hills

Linear features exist on the slopes of streamlined hills (e.g. Fig 4 d). Like the linear ridges on the depression floors, they have shadows on their E sides, but lack relatively brightly illuminated W sides. MOLA data reveal that they have vertical dimensions that are at most only a few metres (e.g. Fig. 4 c). They resemble the sets of steps similar to the linear features on the slopes of the depression margins.

v) ‘Tear-drop’ shaped hills

Hills shaped like tear-drops are common in the study area (e.g. Fig. 4 a, b and d). These cover areas of a few hundred metres to several kilometres or more. Some have formed around pre-existing craters (e.g. Fig. 4 d) whereas others, with less obvious shapes, have formed around low hills (e.g. Fig. 4 a and b). Some of these low hills contain low-relief depressions (e.g. the hill crossed by profiles e’- e and f’- f shown in Figs. 4 a, b, and topographic profiles e’- e and f’- f).

Interpretation of five geomorphic landforms at Location 1:

i) We interpret the depressions visible on the CTX images, and apparent in the MOLA profiles, as channels. We do not think these depressions are cut by the passage of glaciers because their depth to width ratios (40 m x 3000 m) have a form ratio of 0.013 and do not resemble terrestrial examples whose form ratios, for active glacial channels, is between 0.20 and 0.58 (Harbor, 1992). The fact that we have not observed up-standing morphologies like those associated with lavas or mudflow deposits, but instead incised depressions, does not support formation by flowing viscous lava or the passage of mudflows. Aqueous flow at relatively high velocity could produce such incision, but we concede that this does not rule out the flow of turbulent lavas that may also produce mechanical erosion (Jaeger et al. 2010).

ii) We interpret linear features on the channel floor as so-called “longitudinal grooves” or “longitudinal lineations” (Baker 1978, Burr et al. 2002), that have been used to infer catastrophic flow terrain on Earth and Mars (Baker 1978, Baker and Milton 1974). They form due to high flow velocities associated with flowing water, perhaps with some entrained sediment, but turbulent lavas may have also been involved (e.g. Jaeger et al. 2010). In summary, observations imply that the channel-floor landforms were formed by rapid flow by water or turbulent lava.

iii) We interpret the linear features on the depression margin slopes as terraces on channel margin slopes. Burr et al. (2002) interpreted similar terraces as the result of erosion of a pre-existing layered terrain, which may be correct in places. However, here we suggest that they also resemble “bathtub rings” that are cut by high flow velocities and vortices, and left by lowering water levels during waning flows (Baker

1973, 1978). The flow of turbulent lava may also have caused the mechanical erosion (e.g. Jaeger et al. 2010). Note that the interpretations of erosion of pre-existing layered terrain versus recessional terraces may not be mutually exclusive and hence challenging in regions where sub-horizontal lava layers may be present such as Grjótá Valles. For the particular examples we describe, our interpretation is that as the fluids that formed the channels waned, the fluid level dropped cutting terraces into bedrock so they formed during recession of fluids leaving features that resemble bath-tub rings. We use the term "recessional terraces" for these features. We also note that we are unaware of any examples where terraces such as those we have observed are produced by flowing highly-viscous lava or mudflows.

iv) We interpret the linear features on the streamlined hills in the same way that we interpret the linear features on the depression margin slopes. We suggest these are recessional terraces cut by waning rapid fluid flows.

v) Due to the existence of what we interpret as recessional terraces cut by waning rapid fluid flows, we interpret the hills shaped like airfoils as streamlined islands cut by the flows. The most distinctive evidence for rapid fluid flows is the presence in the channels of streamlined mesas, i.e. flat-topped, topographically higher landforms that have a 'tear-drop' shape in planview in which their rounded ends point up slope and their pointed ends down slope (Burr et al., 2002). Such features are clearly visible in Figs 4 a, b, and d notably the impact crater which is a streamlined island through which transect A passes. It displays a classic tear-drop shape, with a generally flat top east of the impact crater with pointed end of the 'tear-drop' pointing downstream. The morphology of the streamlined islands suggests a general flow direction of NW to SE for the example shown in Figure 4 b. Our estimated flow direction is the same in this location, and in fact across our entire study region, as Burr and Parker's (2006) estimates (Figure 1 b).

In summary, we note that Location 1 does not contain landforms reminiscent of highly viscous lava flows or mudflows. We see no examples of (a) ring-mound landforms that some have interpreted as volcanic (rootless) cones (Jaeger et al. 2007), (b) thin, concentric, lobate flow fronts that indicate overlapping lavas (Jaeger et al. 2007), or (c) platy-flow or platy-ridged surfaces indicating lava crusts

(Chapman et al. 2010, Keszthelyi et al. 2000). This suggests to us that the channels and streamlined island were not cut by the passage of highly viscous lava. Instead, as suggested by a number of other authors (e.g. Burr et al. 2002, Jaeger et al. 2010), we interpret the five geomorphic landforms described and interpreted above as evidence for aqueous flow or the flow of turbulent lavas. We also see no landforms reminiscent of other mudflow products such as: (a) hills characterised by circular plan-map appearance with flow like structures extending from their bases,(b) elongated ridges with rough surfaces, (c) wide plateaus with a smooth central uplifted unit, often containing a rimless pit, and (d) an extensive and chaotic combination of overlapping landforms of points (a), (b) and (c) above (Brož, et al. 2020; Cuřín et al., 2021).

Observations of the relative chronology of geomorphic features

The key observation that provides evidence of relative chronology is that the channel that NW-SE cuts across and incises down across other channels that run E-W (Fig. 4b). The base elevation of the E-W channels is about -2156 m, whilst the base elevation the NW-SE channel is deeper, at about -2194 m, implying ~40 m of incision (Fig. 4e topographic profiles a'- a through f'- f). Also, recessional terraces associated with the E-W channels and streamlined islands exist at elevations of -2130 m to -2160 m, above those for the NW-SE channel (-2170 to -2195 m). The recessional terraces from the E-W channels are oblique to and appear to be cross-cut by recessional terraces from the NW-SE channel (e.g. the region between profiles b'- b and c'- c, Fig. 4b).

Interpretation of the relative chronology of geomorphic features

Our interpretation is that two distinct periods of channel formation are visible in Figure 4. The observation that our interpreted recessional terraces from the earlier channels are cross-cut by those associated with the later channel (as is also visible in Figures 2, 5, 6, 7, 8, and 9) suggests that water levels from an initial flow had fully-waned before the later channel started to form. Thus, our interpretations suggest two separate flow events, and the separate channels are not simply anastomosing distributary channels from a single flow.

Channel sources

We mapped the channels back to their sources. The earliest flow can be mapped back to a source located in the current location of the faults, fractures and fissures that form part of Cerberus Fossae (Figure 2 and Figure 3 a and b). The source region is partly surrounded by enclosing cliffs, and flow directions from streamlined islands suggest initial flow towards both the north and the south of the present position of Cerberus Fossae. The walls of the faulted depression appear fresh and un-eroded by the flow, suggesting that the faulting occurred after flow formation, similar to the interpretation of the timing of flows and faulting advanced by Burr et al. (2002) and Vetterlein and Roberts (2009). The later flow can be mapped back to a source, again partly-constrained by enclosing cliffs (Figure 2 and Figure 3 c and d). The source of the second flow is to the east of the source of the earlier flow. Again, the walls of the faulted depression appear fresh and un-eroded by the flow, suggesting that the faulting occurred after flow formation.

Summary

Observations from Location 1 (Figure 4) have been interpreted to indicate the existence of two separate flow events (Flow 1 and Flow 2) that can be mapped back to two separate sources.

Note that we mapped a large number of geomorphic features for the other locations described in this paper. Space does not allow us to separate description and interpretation for every example in the rest of the paper, but we will show that the five types of geomorphic features described above are widespread across the region in Figure 2. We use our observations and interpretations of Location 1 as type examples to guide interpretations of the landforms in Locations 2 through 7 and Supplementary Locations A through D.

Location 2 (Fig. 5)

Location 2, centred at 15.60° N, 162.07° E, is east of Location 1 and shows more examples of cross-cutting relationships between Flow 1 and Flow 2. The channels are characterised by linear features on the channel floors and on the channel margins that we interpret as longitudinal lineations and recessional terraces respectively (Fig. 5c). Landforms from Flow 1 are preserved on top of two streamlined islands defined by Flow 2, and we describe five inter-connected channels that we assign to Flow 2.

Flow 1 has produced multiple channels confined to within the bounds of two streamlined islands. Flow directions during Flow 1 were generally to the NE and SE. We assign them to Flow 1, correlated with the features mapped at Location 1, because one of the streamlined islands exists in both Location 1 and Location 2, and the channels have a similar basal elevation (Location 1, -2180 m: Location 2, -2180 m).

Flow 2 cross-cuts Flow 1 in the following locations. For Flow 2, sub-channels 1 and 2 are tributary channels, flowing north and south of a streamlined island that preserves features from Flow 1; they join to form sub-channel 3. Sub-channel 4 is a distributary channel that diverges from sub-channel 2 as they abut against a streamlined island, upon which features from Flow 1 are preserved. Sub-channel 5 is a distributary channel that diverges from sub-channel 3. At the northern end of transect c'- c (Fig. 5 map 1 and 2) one of the Flow 2 channels, sub-channel 3, flows towards the SE and cuts across a channel associated with Flow 1. The base of sub-channel 3 incises downwards to -2295 m, ~40 m beneath the basal elevation of channels associated with this portion of Flow 1 at around -2255 m and also beneath recessional terraces of Flow 1 (Fig. 5, topographic profile c'- c).

Flow 2 also incises down below the level of Flow 1. On transect c'- c (Fig. 5, topographic profile c'- c) the elevation difference between the base of the second channel and the recessional terraces from Flow 1 suggest incision of up to ~40 m. MOLA transect D (Fig. 5, maps A and B) crosses sub-channels 3 and 5 from Flow 2. Both topographic data and recessional terrace markings show that the Flow 2 channel (sub-channel 3) has incised down beneath the elevation of Flow 1. The incision is approximately 40 metres, from -2250 m to -2290 m, and these values are similar to those derived from transect c'- c. The distributary Flow 2 channel (sub-channel 5) has incised down into the surface produced by Flow 1. The incision is approximately 10 metres, from -2250 m to -2260 m. Evidence that Flow 2 incises beneath the level of

Flow 1 can also be seen in topographic profiles a'- a and b'- b, with values for incision of ~35 m and ~15 m respectively.

In summary, Location 2 contains evidence for the two separate flows. Mapping back to the sources of the flows indicates that these are the same two flows identified at Location 1.

Location 3 (Fig. 6)

Location 3 (Fig. 6), centred at 15.58° N, 162.37° E, again reveals more details of the relationship between Flows 1 and 2, and is downstream of Location 2, where we might expect incision from Flow 2 to be greater. Flow 1 landforms are correlated with those in Locations 1 and 2 because its base elevation is similar to that in those areas (-2270 to -2290 m) and a streamlined island upon which Flow 1 landforms exist is continuous between Locations 2 and 3. Like Locations 1 and 2, the floors and margins of channels are characterised by longitudinal lineations and recessional terraces (Fig. 6c).

Within a streamlined island, a broad Flow 1 channel shows longitudinal lineations and streamline features indicating flow towards the east and NE, with evidence for waning flow in the form of recessional terraces. A later flow (Flow 2) channel flowed towards the SE, and in so doing cross-cut the Flow 1 channel landforms. The base elevation for the Flow 1 channel ranges from -2270 m in the west (MOLA transect a'- a), to -2290 m in the east (MOLA transect d'- d) (Fig. 6, topographic profiles a'- a and d'- d). Flow 2 cross-cuts Flow 1 and a series of clear recessional terraces are found across the area of cross-cut. The orientation of these Flow 2 recessional terrace marks are perpendicular to the flow direction of Flow 1 and its recessional terraces. The extent of the Flow 2 incision decreases from west to east, with a maximum incision of approximately 70-75 metres at MOLA transect a'- a, ~60 metres at MOLA transect b'-b, ~50 metres at MOLA transect c'- c, and ~35 metres at MOLA transect d'- d, in tandem with the decreasing basal elevation of the Flow 1 channel features. The fissures are clearly younger geological features, as flow from Flow 2 is to the SE on both sides of the fissure, appearing to have been cut by the fissure, so the recessional terrace markings from the flows were disrupted by later faulting.

In summary, Location 3 contains evidence for the two separate flows. Mapping back to the sources of the flows indicates that these are the same two flows identified at Location 1.

Location 4 (Fig. 7)

Location 4, centred at 15.60° N, 162.75° E, is located to the east of the previous three Locations, and focuses on a relatively early channel, possibly from Flow 1, that is cross-cut by a third flow, Flow 3. Again, these channels are characterised by longitudinal lineations and recessional terraces (Fig. 7c).

Recessional terrace marks from a relatively early channel, together with MOLA data from transects a'- a, b'- b and c'- c, suggest that a flow channel, possibly Flow 1, flowed from the west to the north-east, with the base elevation for this channel being approximately -2310 to -2320 m (Fig. 7 maps 1 and 2, and topographic profiles a'- a, b'- b and c'- c). We believe this may be a remnant of Flow 1 that was not covered by Flow 2, because the base levels of the channels at -2315 m appear to be the downward continuation of those for Flow 1 at Location 3 (around -2290 m), rather than a continuation of those for Flow 2 which are lower in elevation (around -2345 m) (see Figure 11 for a compilation of elevations).

At Location 4, the later flow cannot be mapped back to flow source 2. Instead, the later flow is interpreted to be a third flow, Flow 3, because it can be mapped back to a source shown in Figures 2 and Figure 3 e and f. This source is again located along the trace of Cerberus Fossae, and faulting appears to post-date the flow because the walls of the subsided fault, fracture and fissure system appear un-eroded by the food. The source is again partially surrounded by enclosing cliffs. Flow 3 incises downwards into the earlier flow by between ~7 m to 25 m.

Location 5 (Fig. 8)

Location 5, centred at 15.13° N, 163.21° E, is located further to the east and shows an area with three possible flow channels, two exhibiting cross-cutting relationships (Fig. 8 maps 1 and 2). We suggest that a fourth flow, Flow 4, can be identified at this location because it can be mapped back to a separate source (Figures 2 and 3 g and h). Again, these channels are characterised by longitudinal lineations and recessional terraces (Fig. 8c).

Beginning with the oldest flow features, we find recessional terrace markings along two of the MOLA transects at relatively high elevations: c'- c and e'- e. The topographic profiles for these transects (Fig. 8 maps 1 and 2, and topographic profiles c'- c and e'- e) indicate that recessional terraces at elevations of -2325 m and -2340 m are located high on the escarpment running SW-NE across the image (Fig 8, map 2, indicated by white arrows). We attribute these terrace markings to Flow 2. A later flow incised downwards, and this incision cut a channel down to -2370 m (Fig. 8, transects d'- d and e'- e) and we suggest this is a remnant of the Flow 3 channel, untouched by the later Flow 4. Flow 4 incises more deeply, with the base of its channel at a depth of approximately -2379 metres (transect a'- a), to a maximum of -2390 metres (transect c'- c). Recessional terrace markings indicating the flow for Flow 4 was ~20 m deep (Fig. 8 transect b'- b).

We interpret the existence of Flow 4 because the channels we attribute to it can be mapped back to a source ~15 km to the NW (see Fig. 2 and Fig. 3g and 3h). The source is a depression along the trace of Cerberus Fossae that is partially enclosed and defined by surrounding cliffs. The sidewalls of the fossae cross-cut the enclosing cliffs indicating that the faulting is later than the flowing.

This location is the only one where we have identified with possible examples of rootless cones (Fig.9b). However, these are adjacent to a later fissure, and are not present over the majority of the channel floor. Our interpretation is that the rootless cones, if that is what they are, are related to a relatively small lava flow associated with the later fissure system, and hence were not responsible for channel formation because their associated lava post-dates channel formation.

Location 6 (Fig. 9)

Location 6, centred at 15.60° N, 163.30° E, focuses on a small hummocky location just to the north of the main W to E fissure that cuts across the central Regional Map

(Fig. 2). The location is 20 km to the NNE of the source of Flow 4, and approximately 40 km to the NE of the source of Flow 3 (Fig. 2). We interpret this area to show a cross-cutting relationship between a Flow 4 channel and earlier Flow 3 channels. There may also be remnant recessional terraces from a Flow 2 channel. Again, these channels are characterised by longitudinal lineations and recessional terraces (Fig. 9c).

Location 6 illustrates how Flow 3 channels flowed around, through and possibly to the south of the two areas of higher ground (Fig. 9). MOLA transects a'- a and b'- b show that what is probably the base of the Flow 3 channel was at approximately -2360 metres, and recessional terrace marks are visible up to about -2320 metres, indicating that the vertical extent of this Flow 3 channel was in the region of 33 m to 35 m at these locations. MOLA transects c'- c, d'- d and e'- e are challenging to interpret because they pass through an area that divides the two areas of high ground. The presence of recessional terrace marks suggests that a channel from Flow 3 may have flowed in a south to north direction up between the two areas of high ground. If this were the case, and we can measure the height of Flow 3 using the base elevation of the channel as -2355 metres. Interpretation of the MOLA transects c'- c, d'- d and e'- e suggests that the maximum elevation of Flow 3 was about -2290 metres, meaning that the vertical extent of this Flow 3 channel at this location was ~65 metres.

We believe a later flow incised across the channel from Flow 3, as shown in Figure 9, maps 1 and 2). This flow can be mapped back to a source (Fig. 2 and Fig. 3 g and 3h), identifying it as from Flow 4. A Flow 4 channel runs west to east at the bottom of Fig. 9, map 2 with a base elevation of approximately -2380 metres, incising below the base of Flow 3 by up to ~45 m. Recessional terrace marks for the Flow 4 channel were identified on all MOLA transects, with the depth of the Flow 4 channels ranging from ~40 m (a'- a), ~20 m (b'- b and c'- c) to only being able to identify the recessional terrace marks of Flow 4 (d'- d and e'- e). A small area in Fig. 9, map 2, shows a possible remnant area of a Flow 2 channel. The lowest identified recessional channel for this possible Flow 2 channel area was at about -2270 metres, and the highest identified recessional channel for this possible Flow 2 channel area was at about -2220 metres. If this is indeed a Flow 2 channel remnant, the vertical extent of the flow would have been well in excess of 50 metres.

Formation of the fossae took place after the flow episodes, with the fissures cross-cutting the recessional terrace markings of the flows, with the new fissure formations running parallel with the major fissure running through this region, approximately 16 km to the south-west of the newly formed fissure.

Location 7 (Fig. 10)

Location 7, centred at 15.46° N, 163.28° E, is an extension of Location 6 (Fig. 9), to the south, focuses on the relationship between Flows 3 and 4. As with Location 6 (Fig. 9), Location 7 is a hummocky area with one clear and discernible flow channel running north-east then east through the middle of the location map. There are smaller channels to the south of the map, notably a clear channel flowing in a north-easterly direction. Again, these channels are characterised by longitudinal lineations and recessional terraces (Fig. 10c).

The centre of Location 7 is just 15 km to the north-east of the estimated source area of Flow 4. The main channel from Flow 4 traces a path north-east across Figure 10 maps 1 and 2, cross-cutting earlier flow channels formed by Flow 3. The base elevation of the main Flow 4 channel appears to deepen moving west to east. Topographic profiles a'- a and b'- b reveal a base elevation of approximately -2365 metres, which deepens to approximately -2380 metres in topographic profiles c'- c, d'- d and e'- e. Recessional terrace marks for Flow 4 suggest that the upper limit for Flow 4 in this area was between -2330 metres and -2340 metres, meaning that the vertical extent of Flow 4 ranged from approximately 25 metres (topographic profiles a'- a and b'- b), to between ~50 metres and ~25 metres (topographic profiles c'- c, d'- d and e'- e). Recessional terrace markings for an earlier flow are visible and are suggested to be Flow 3 recessional terraces based on the MOLA data that define the base of interpreted Flow 3 channels at similar elevations in different locations (e.g. -2325 m in Location 4, Fig. 7; -2335 m in Location 7, Fig. 10). Data regarding the possible source elevation of Flows 3 and 4 (Fig. 11) shows the Flow 3 source to be at -2325 metres and the Flow 4 source to be at -2344 metres. These measurements suggest that the recessional terrace markings and geomorphic features observed in Location 7 maps 1 and 2 (Fig. 10) and accompanying topographic profiles, above -2330 metres are very probably Flow 3 markings and formations. The Flow 4 source elevation is -2344 m, and therefore recessional marks at this elevation and below are most likely formed by Flow 4. Measurements are consistent with the incision depth of Flow 4 (just over -2380 metres), which we have calculated is the base elevation for Flow 4 in this location.

There are possibly four remnant Flow 3 areas within the Flow 4 area, but they do not show clear cross-cutting relationships with Flow 4 and ascertaining a base elevation for Flow 3 in this region is challenging using available MOLA data because the coverage is sparse and does not include the locations that would possibly show clear cross-cutting relationships. MOLA data from Location 6 (Fig. 9), on the northern section of the area within Location 7 (Fig. 10), reveals a base elevation of Flow 3 as -2365 metres. However, that measurement is for the northern channel of Flow 3 and is distinct from the Flow 3 channel we are focused on in this image, i.e. the channel to the south of the split-hill formation in the north of Location 7 maps 1 and 2 (Fig. 10). Nevertheless, the measurement can be used as a useful proxy and does suggest that the Flow 4 channel measured here is in fact Flow 4 and not Flow 3 although the possibility does exist that we may have overestimated the vertical extent of Flow 4 in this region because the region is not comprehensively covered by MOLA transects.

Supplementary Locations A through D (Figs. S1 through S4)

A further four locations were identified that provided further evidence and examples of landforms in downstream locations that may have been produced by flows. The four location figures and landforms are discussed in greater detail in the Supporting Information, Supplementary Locations A through D (figs. S1 through S4) and these locations are also highlighted on Figure 2 as SL. A, SL. B, SL. C, and SL. D.

Construction of a regional map and channel profiles

The Regional Map (Fig. 2), centred at 15.25° N, 162.85° E, and overall channel profiles (Figure 11) attempt to draw all the data gleaned from locations and supplementary locations into a whole, to gain a regional overview of the flow geometries. The regional map covers the area of the northernmost Cerberus Fossae, a ~197 km long set of *en* *echelon* fissure segments that run west by north to east by south, as well as part of the unnamed northern channel system to the north and east, and the scoured area to the south and east of the northernmost Cerberus Fossae.

We believe that five separate flow episodes can be identified in our regional map (Fig. 2). The cross-cutting relationships identified indicate that the fissures and fractures associated with Cerberus Fossae appear to have formed after the flow episodes.

The first, Flow 1, with its source at the far west of the northernmost Cerberus Fossae at an approximate elevation of -2139 m, appears to be the largest in terms of area covered. This was followed, after an unknown period of time, by Flow 2, with its source further east and at an approximate elevation of -2165 m. The cross-cutting relationships between Flow 1 and Flow 2 are the clearest, with Locations 1, 2 and 3 showing unambiguous evidence of the existence of two distinct flow episodes in this area. Moving further east, we find the source of Flow 3 at an approximate elevation of -2325 m, with the source of Flow 4 at an approximate elevation of -2345 m. Locations 4, 5, 6 and 7 (Figs. 7, 8, 9, and 10) cover the Flow 3 region, with Location 4 looking at the Flow 1 / Flow 3 relationship, and Locations 5, 6, and 7 (Figs. 8, 9, and 10) looking at the Flow 3 / Flow 4 relationship. The source of Flow 5 is at an approximate elevation of -2451 m, and is the final flow source we have identified. We observe that the channel rises very slightly by approximately 8m before plateauing out and then flowing downward eastward. We have been unable to unambiguously define a cross-cutting relationship with Flow 4, hence we chose to put this location in our Supplementary Locations files (Supplementary Location D (Fig. S4). However, as explained in regard to Supplementary Location D (Fig. S4), we are confident that this is the source area of a separate flow (Flow 5), primarily due to geomorphic indicators that reveal flow direction and the geomorphology of the source with enclosing cliffs.

Figure 11 shows the location (elevation and longitude) of each flow (Flow 1 through 5) at source. We then connected the base elevation of each channel (1 through 4) at each location (L1 through L7) to the location of each flow source. Each of the five flow sources (Flow 1 through 5) occurs progressively further to the east, with the elevation of each source progressively lower from west to east. A key observation is that the channels from these five sources all flow downhill from west to east. Where cross-cutting relationships have been identified and described above, each channel is at a lower elevation and hence incises downwards into it predecessor channel.

In summary, our results indicate that the study area was affected by a sequence of multiple flows emanating from at least five sources that appear to be located progressively further to the east along the direction of the northernmost Cerberus Fossae. Each flow event flowed downhill and each flow source occurs at progressively lower elevations (Fig. 11 A and B).

Discussion:

Prior to our study, discussions of the geology of the region of Grjótá Valles were focussed on the following: (1) Extensive channels exist that emanate from the vicinity of faults, fractures and fissures that form part of Cerberus Fossae. (2) There had been some suggestions that multiple channels may exist, this was still an open question (Burr and McEwen 2002; Burr et al. 2002; Burr et al. 2006). (3) Channel formation processes had not been conclusively determined, with the debate still open (Burr et al. 2002, Leverington 2004, 2012, Jaeger et al. 2010). (4) Faulting post-dates channel formation evidenced by the un-eroded fracture walls, bi-directional flow directions at some flow sources, and fractures cross-cutting channels (Vetterrlein and Roberts 2009). (5) Evidence for palaeoseismic marsquakes has been gathered using observations of mobilised boulder populations (Brown and Roberts 2019). (6) Seismicity associated with normal faulting marsquakes had been recorded in the vicinity by the InSight seismometers (Burr et al. 2002, Burr and Parker 2006; Jaeger et al. 2007, 2010, Leverington 2011, Brown and Roberts 2019, Voight and Hamilton 2018, Giardini et al. 2020, Golder et al. 2020). Furthermore, Keske et al. (2015), studying ouflow channels elsewhere on Mars noted that there exists a ‘close interplay of fluvial and volcanic activity’ which would suggest ‘…that fluvial activity not only played a major role during a period of volcanism, but also may be linked to, or even triggered by, volcanic processes’. We note that if the eastward progression in channel formation is due to fault or dike propagation then in the past the distribution of seismicity would have changed through time, and this should be considered when developing models to explain the present-day seismicity.

Our results provide insights into the above because they document clear cross-cutting relationships between flow channels which can be mapped back by to five distinct flow sources, with the locations of sources progressively located further to the east through time. Our observations confirm that the flows that formed the channels pre-dates surface faulting. If igneous processes are responsible for triggering the flows, then these processes acted before faulting appeared at the surface, and hence this may or may not predate the onset of the present-day seismicity. This sequence is not unexpected, as the idea that injection of sub-surface dikes leads to the formation of overlying graben has been modelled (Rubin 1992) and observed (Wright et al. 2006) in terrestrial examples, with these ideas widely applied to graben on Mars. Indeed, the heating produced by dike injection has been suggested to provide the possibility of melting sub-surface ice, or releasing water trapped by ice (McKenzie and Nimmo 1999, Head et al. 2003). However, the issue has been that the large geographic extent of the channels, for example associated with Grjótá Valles, have been taken to suggest very large volumes of fluid, and hence flow-rates that may be implausibly high (Head et al. 2003, Leverington 2011). If the dimensions of the active channel is smaller than that implied by a single larger channel, then the flow rates may also be proportionately lower. However, our lack of knowledge on the flow duration and composition of the flow limit our ability to state a specific flow rate. Furthermore, observations from the InSight seismometers suggest that the seismic velocity below 10 km for Elysium Planitia is too low to be ice-saturated (Manga and Wright 2021).

Although It is clear that more work is needed to explain the links between igneous processes, faulting, seismicity, water/ice in the crust and formation of flow channels by water and/or turbulent lava, it is interesting that our results imply relatively small flows compared to previous estimates. This is because the total geographic extent of the channel system associated with Grjótá Valles was formed by at least five distinct flows, not a single event. Despite this conclusion, unfortunately we have no way to quantify the volume or the flux rate of fluid discharge due a lack of knowledge regarding the duration of each single flow event. Another interesting aspect is that the flow sources are located progressively further to the east through time. We have been unable to provide more data that constrain the process or processes that liberated the fluids, but we do provide the insight that those processes propagate to the east through time. One possibility is that eastward propagation of fluid release, if produced by melting due to intrusion of sub-surface dikes, or eruption of turbulent lava, may suggest eastward dike propagation as is speculatively shown in Figure 12. Another alternative is that intrusion of dikes occurred progressively further east, but emanated from a sub-surface volcanic source that already underlay the region (Genova et al., 2016, Golder et al., 2020). Although we have no direct constraints on the time scale of this propagation we note that Golder et al. (2020) provide crater count ages that become progressively younger towards the east (53 Ma, then 33 Ma, then 31 Ma) in the region we study. They suggest the change in apparent age is caused by the changes in rheological properties of the lavas during emplacement, such as material strength and porosity. Although we have no grounds to dispute this explanation, we note that the ages are obtained from areas that partially overlap the flow deposits (Fig. 1b), and the age of 53 Ma coincides within the proximal regions for Flow 1 and Flow 2, the 33 Ma age coincides with the region occupied by the distal parts of our Flow 3 and Flow 4, and the 31 Ma age coincides with a region to the east of the area we have mapped that may be occupied by Flow 5. We suggest that more work may be warranted to clarify the geological significance of crater counts in Grjótá Valles as this may help elucidate the timing of the relationships between volcanic, aqueous, faulting and seismicity processes in this enigmatic region.

Conclusions:

We conducted a detailed analysis of the northernmost Cerberus Fossae and the surrounding area using CTX images, HiRISE images and MOLA data. Our conclusions are as follows.

1. Examination of the floors and margins of prominent channels reveal the presence of landforms such as channel floor longitudinal lineations and channel margin recessional terraces that appear to have been cut by water and/or turbulent lava, with no signs of landforms that would suggest that the channels have been cut by viscous lava or mudflows.

2. Cross-cutting relationships and channel incision reveal at least five asynchronous flow episodes have taken place, sourced at different locations along a 180 km section of the main northernmost Cerberus Fossae, demonstrating that the channels were formed by multiple events.

3. Channels flow downhill away from the sources we have identified, with younger channels cross-cutting older channels, incising downwards by 25 m to 70 m.

4. The source areas for the flows are located progressively further to the east through time.
5. We have been unable to explain the eastward progression of flow sources, but we suggest that possibilities may include either dike propagation from west to east which melted near-surface ice, or released turbulent lava, or that magma from an underlying regional melt zone influenced melting of ice near the surface further to the east through time.
6. Further work is required to elucidate the mechanisms responsible for the release of fluids; however, our observations show that whatever the explanation, the mechanism does not need to produce the large volumes of fluid implied if the channels are all interpreted to have formed asynchronously.

Acknowledgements:

This work was part of a self-funded PhD study by Brown. Roberts acknowledges STFC grant ST/K006037/1 in the initial part of this work. A Data Availability Statement is available for this paper, with all data used being available through Figshare. We thank the Editors, Susan Conway and several anonymous reviewers for comments that improved the paper.

Data Availability Statement:

We acknowledge the use of imagery provided by services from NASA's Mars Reconnaissance Orbiter (MRO), and MOLA Precision Experiment Data Records (PEDRs). We acknowledge the use of Google Earth in our research. All data are available in Brown and Roberts (2022)

References:

Albee, A.L. *et al.* (2001) “Overview of the mars global surveyor mission,” *Journal of Geophysical Research: Planets*, 106(E10), pp. 23291–23316. Available at: https://doi.org/10.1029/2000je001306.

Baker, V.R. (1973) “144 : Paleohydrology and sedimentology of Lake Missoula flooding in Eastern Washington,” *Geological Society of America Special Papers* [Preprint]. Available at: https://doi.org/10.1130/spe144.

Baker, V.R. and Milton, D.J. (1974) “Erosion by catastrophic floods on Mars and Earth,” *Icarus*, 23(1), pp. 27–41. Available at: https://doi.org/10.1016/0019-1035(74)90101-8.

Baker, V.R. and Patton, P.C. (1978) “New evidence for pre-wisconsin flooding in the channeled scabland of Eastern Washington,” *Geology*, 6(9), p. 567. Available at: https://doi.org/10.1130/0091-7613(1978)6<567:nefpfi>2.0.co;2.

Berman, D.C. and Hartmann, W.K. (2002) “Recent fluvial, volcanic, and tectonic activity on the Cerberus Plains of Mars,” *Icarus*, 159(1), pp. 1–17. Available at: https://doi.org/10.1006/icar.2002.6920.

Brown, J.R. and Roberts, G.P. (2019) “Possible evidence for variation in magnitude for marsquakes from fallen boulder populations, Grjota Valles, Mars,” *Journal of Geophysical Research: Planets*, 124(3), pp. 801–822. Available at: https://doi.org/10.1029/2018je005622.

Brown, J.R. and Roberts, G.P. (2022) *Repeated, cross-cutting and spatially migrating outflow channel formation, Grjótá Valles, Mars*, *figshare*. figshare. Available at: https://figshare.com/collections/Repeated_cross-cutting_and_spatially_migrating_outflow_channel_formation_Grj_t_Valles_Mars/5794766 (Accessed: December 26, 2022).

Brož, P. *et al.* (2020) “Experimental evidence for lava-like mud flows under martian surface conditions,” *Nature Geoscience*, 13(6), pp. 403–407. Available at: https://doi.org/10.1038/s41561-020-0577-2.

Burr, D.M. and McEwen, A.S. (2002) *The extremes of the extremes: Extraordinary floods: Proceedings of an international symposium on extraordinary floods held at Reykjavik, Iceland, in July 2000*. Wallingford: International Association of Hydrological Sciences. Recent Extreme Floods on Mars. pg. 101.

Burr, D.M. and Parker, A.H. (2006) “Grjotá Valles and implications for flood sediment deposition on Mars,” *Geophysical Research Letters*, 33(22). Available at: https://doi.org/10.1029/2006gl028011.

Burr, D.M. *et al.* (2002) “Repeated aqueous flooding from the Cerberus Fossae: Evidence for very recently extant, deep groundwater on Mars,” *Icarus*, 159(1), pp. 53–73. Available at: https://doi.org/10.1006/icar.2002.6921.

Burr, D.M., Sakimoto, E.H. and McEwen, A.S. (2002) "Recent aqueous floods from the Cerberus Fossae, Mars," *Geophysical Research Letters*, 29(1). Available at: https://doi.org/10.1029/2001gl013345.

Burr, D.M., Wilson, L. and Bargery, A.S. (2009) "Floods from fossae: A review of Amazonian-aged extensional–Tectonic Megaflood channels on Mars," *Megaflooding on Earth and Mars*, pp. 194–208. Available at: https://doi.org/10.1017/cbo9780511635632.010.

Carr, M.H. (1979) "Formation of martian flood features by release of water from confined aquifers," *Journal of Geophysical Research*, 84(B6), p. 2995. Available at: https://doi.org/10.1029/jb084ib06p02995.

Chapman, M.G. *et al.* (2010) "Amazonian geologic history of the Echus Chasma and Kasei Valles System on Mars: New data and interpretations," *Earth and Planetary Science Letters*, 294(3-4), pp. 238–255. Available at: https://doi.org/10.1016/j.epsl.2009.11.034.

Cuřín, V. *et al.* (2021) "Mud flows in the southwestern Utopia Planitia, Mars." Available at: https://doi.org/10.5194/epsc2021-382.

Genova, A. *et al.* (2016) "Seasonal and static gravity field of Mars from MGS, Mars Odyssey and Mro Radio Science," *Icarus*, 272, pp. 228–245. Available at: https://doi.org/10.1016/j.icarus.2016.02.050.

Giardini, D. *et al.* (2020) "Seismicity of Mars," *Nat. Geosci.*, (13), pp. 205–212. Available at: https://doi.org/10.5194/egusphere-egu2020-20437.

Golder, K.B., Burr, D.M. and Kattenhorn, S.A. (2020) "Investigation of target property effects on crater populations in long lava flows: A study in the Cerberus Region, Mars, with implications for magma source identification," *Icarus*, 335, p. 113388. Available at: https://doi.org/10.1016/j.icarus.2019.113388.

Hamilton , C.W. (2013) *Flood lavas associated with the Cerberus Fossae 2 unit in elysium ...* Lunar and Planetary Institute Science Conference Abstracts. vol. 44. pp. 3070. Available at: https://www.researchgate.net/publication/258804346_Flood_Lavas_Associated_with_the_Cerberus_Fossae_2_unit_in_Elysium_Planitia_Mars (Accessed: December 26, 2022).

Harbor, J.M. (1992). Numerical modeling of the development of U-shaped valleys by glacial erosion. *Geological Society of America Bulletin*, *104*(10), 1364–1375. https://doi.org/10.1130/0016-7606(1992)104<1364:nmotdo>2.3.co;2

Hartmann, W.K. and Berman, D.C. (2000) “Elysium Planitia Lava Flows: Crater count chronology and geological implications,” *Journal of Geophysical Research: Planets*, 105(E6), pp. 15011–15025. Available at: https://doi.org/10.1029/1999je001189.

Head, J.W., Mitchel, L.K. and Wilson, L. (2003) “Generation of recent massive water floods at Cerberus Fossae, Mars by dike emplacement, cryospheric cracking, and confined aquifer groundwater release,” *Geophysical Research Letters*, 30(11). Available at: https://doi.org/10.1029/2003gl017135.

Jaeger, W.L. *et al.* (2007) “Athabasca Valles, Mars: A lava-draped channel system,” *Science*, 317(5845), pp. 1709–1711. Available at: https://doi.org/10.1126/science.1143315.

Jaeger, W.L. *et al.* (2010) “Emplacement of the youngest flood lava on Mars: A short, turbulent story,” *Icarus*, 205(1), pp. 230–243. Available at: https://doi.org/10.1016/j.icarus.2009.09.011.

Jones, A.P. *et al.* (2011) “A geomorphic analysis of Hale Crater, Mars: The effects of impact into ice-rich crust,” *Icarus*, 211(1), pp. 259–272. Available at: https://doi.org/10.1016/j.icarus.2010.10.014.

Kattenhorn, S.A. and Meyer, J.A. (2010) *Magmatic dikes and megafloods: A protracted history of interactions ...* Available at: https://www.researchgate.net/publication/270572954_Magmatic_dikes_and_megafloods_a_protracted_history_of_interactions_between_magma_and_subsurface_ice_Cerberus_Fossae_Mars (Accessed: December 26, 2022).

Keske, A.L. *et al.* (2015) “Episodes of fluvial and volcanic activity in Mangala Valles, Mars,” *Icarus*, 245, pp. 333–347. Available at: https://doi.org/10.1016/j.icarus.2014.09.040.

Keszthelyi, L., McEwen, A.S. and Thordarson, T. (2000) “Terrestrial analogs and thermal models for martian flood lavas,” *Journal of Geophysical Research: Planets*, 105(E6), pp. 15027–15049. Available at: https://doi.org/10.1029/1999je001191.

Keszthelyi, L.P. *et al.* (2007) “Initial insights from 2.5D hydraulic modeling of floods in Athabasca Valles, Mars,” *Geophysical Research Letters*, 34(21). Available at: https://doi.org/10.1029/2007gl031776.

Leverington, D.W. (2004) “Volcanic rilles, streamlined islands, and the origin of outflow channels on Mars,” *Journal of Geophysical Research*, 109(E10). Available at: https://doi.org/10.1029/2004je002311.

Leverington, D.W. (2006) “Volcanic processes as alternative mechanisms of landform development at a candidate Crater-Lake site near Tyrrhena Patera, Mars,” *Journal of Geophysical Research*, 111(E11). Available at: https://doi.org/10.1029/2004je002382.

Leverington, D.W. (2011) “A volcanic origin for the outflow channels of Mars: Key evidence and major implications,” *Geomorphology*, 132(3-4), pp. 51–75. Available at: https://doi.org/10.1016/j.geomorph.2011.05.022.

Leverington, D.W. (2018) “Is Kasei Valles (Mars) the largest volcanic channel in the solar system?,” *Icarus*, 301, pp. 37–57. Available at: https://doi.org/10.1016/j.icarus.2017.10.007.

Manga, M. (2004) “Martian floods at Cerberus Fossae can be produced by groundwater discharge,” *Geophysical Research Letters*, 31(2). Available at: https://doi.org/10.1029/2003gl018958.

Manga, M. and Wright, V. (2021) “No cryosphere-confined aquifer below insight on Mars,” *Geophysical Research Letters*, 48(8). Available at: https://doi.org/10.1029/2021gl093127.

McKenzie, D. and Nimmo, F. (1999) “The generation of martian floods by the melting of ground ice above Dykes,” *Nature*, 397(6716), pp. 231–233. Available at: https://doi.org/10.1038/16649.

Morgan, G.A. *et al.* (2013) “3D reconstruction of the source and scale of buried young flood channels on Mars,” *Science*, 340(6132), pp. 607–610. Available at: https://doi.org/10.1126/science.1234787.

Plescia, J.B. (2003) “Cerberus Fossae, Elysium, Mars: A source for lava and water,” *Icarus*, 164(1), pp. 79–95. Available at: https://doi.org/10.1016/s0019-1035(03)00139-8.

Rubin, A.M. (1992) “Dike-induced faulting and graben subsidence in volcanic rift zones,” *Journal of Geophysical Research: Solid Earth*, 97(B2), pp. 1839–1858. Available at: https://doi.org/10.1029/91jb02170.

Tanaka, K.L., Skinner, J.A. and Hare, T.M. (2005) “Geologic map of the Northern Plains of Mars,” *Scientific Investigations Map* [Preprint]. Available at: https://doi.org/10.3133/sim2888.

Vaucher, J. *et al.* (2009) “The volcanic history of Central Elysium Planitia: Implications for martian magmatism,” *Icarus*, 204(2), pp. 418–442. Available at: https://doi.org/10.1016/j.icarus.2009.06.032.

Vetterlein, J. and Roberts, G.P. (2009) “Postdating of flow in Athabasca Valles by faulting of the Cerberus Fossae, Elysium Planitia, Mars,” *Journal of Geophysical Research*, 114(E7). Available at: https://doi.org/10.1029/2009je003356.

Voigt, J.R.C. and Hamilton, C.W. (2018) “Investigating the volcanic versus aqueous origin of the surficial deposits in eastern Elysium Planitia, Mars,” *Icarus*, 309, pp. 389–410. Available at: https://doi.org/10.1016/j.icarus.2018.03.009.

Captions:

Figure 1. a. Regional location map of the study area, with the locations of Athabasca Valles, and Marte Vallis highlighted. **b.** The study area marked by a black rectangle, to the east of the Elysium Rise. Estimated locations of three Marsquakes (Giardini, et al. (2020) have been added (S0173a, S0183a, and S0235b) as coloured ellipses. Extent of the Grjótá Valles flow tract (after Burr & Parker (2006) has been added. Red lines mark the fossae, with the northernmost being the centre of our study region, and the two to the south-west being the Northern and Southern Cerberus Fossae. Black dots identify two locations that show the approximate paleomarsquakes locations along the Northern Cerberus Fossae after Brown and Roberts (2019). The three white ellipses are crater count locations and their matching crater count model ages for lava flows in this area (Golder et al., 2020).

Figure 2. Regional Map (centred at 15.25° N, 162.85° E) of the study area marking the source areas of the five flows and the extent of each flow. The key study locations, 1 through 7 (Figures 4 through 10 respectively) are shown with white rectangles with L.1, L.2 and so on next to the boxes. Supplementary Locations A through D are shown with white rectangles with SL.A, SL.B and so on next to the boxes. Below the Regional Map are five spot height topographic profiles for the extent of each of the Flow areas 1 through 5 (kilometres / elevation) showing the downward-east sloping topography of the Regional Map area. The vertical exaggeration for each topographic profile is x200.

Figure 3: Panels a. through j. show the approximate location of the source area for each flow (marked and unmarked), marked by a number (1, 2, 3, 4 and 5, representing each flow) in a yellow hexagon. (Panel a. – Flow 1, centred at 16.05° N, 160.48°E / panel c. – Flow 2, centred at 15.56° N, 161.33°E / panel e. – Flow 3, centred at 15.30° N, 162.41°E / panel g. – Flow 4, centred at 15.20° N, 163.05°E / panel j. – Flow 5, centred at 14.56° N, 164.17°E). The source areas have been disrupted by later faulting. Solid blue lines represent enclosing cliffs/boundaries which we are fairly certain about; dashed blue lines represent enclosing cliffs/boundaries which we are less certain about.

Figure 4: Maps and topographic profiles of Location 1 centred at 15.70° N, 161.61°E showing details of channels and cross-cutting relationships (see Figure 2 for location). (a) Map with CTX mosaic with MOLA transects; (b) Map with CTX mosaic with MOLA transects (black lines a'- a through f'- f) and interpreted channel markings/flow directions/recessional terrace markings. Topographic profiles a'- a through f'- f for each of the six transects with the blue line in each graph representing the MOLA transects. (c) Inset from CTX shows detail of the channel floor. Linear features seen on the channel margin slope and the linear features observed on the channel floor do not resemble lava flow landforms such as the presence of thin, concentric, lobate flow fronts that indicate overlapping lavas, or rootless cones. Our interpretation is that they resemble “longitudinal grooves” or “longitudinal lineations” that have been used to infer catastrophic flow terrain on Earth and Mars (Baker 1978, Burr et al. 2002), and/or turbulent lava (Jaeger et al. 2010), and resemble “bathtub rings” that are cut by high flow velocities and vortices, and left by lowering fluid levels during waning flows (Baker 1973, 1978); we term the latter “recessional terraces”. (d) Map showing similar linear features around a streamlined island. (e) Topographic profiles from MOLA spot heights (labelled a'- a through f'- f and located on (a) and (b)) showing the morphologies of channels and craters, and locating linear features on channel margins. The vertical exaggeration for each topographic profile is x50. Overall, for Location 1 our interpretation is that Flow 1 (that flowed from west to east / south-east) is cross-cut by channels formed by a later flow, Flow 2 (that flowed towards the SE). Flow sources are shown in Figure 3.

Figure 5: Maps and topographic profiles of Location 2 centred at 15.60° N, 162.07° E showing details of channels and cross-cutting relationships (see Figure 2 for location). (a) Map 1 – CTX mosaic with MOLA transects. (b) Map 2 – CTX with MOLA transects (black lines a'- a through d'- d) and interpreted channel markings/flow directions/recessional terrace markings. (c) Inset map located in (a) from HiRISE Image ESP_026356_1960 showing details of a channel margin and channel floor. We interpret the presence of longitudinal lineations and recessional terraces (see caption of Figure 4). Talus slopes cover the channel margin in the NE. We have not identified features that would indicate lava flows such as lobate flow fronts or rootless cones. (d) Topographic profiles a'- a through d'- d for each of the four transects with the blue line in each profile representing the MOLA transects. The vertical exaggeration for each topographic profile is x70. Our overall interpretation of Location 2 is that older Flow 1 channels are cross-cut by later Flow 2 channels. Five distinct Flow 2 channels are visible from the maps and topographic profiles. Of interest is the island-like streamlined landform in the top left of Maps 1 and 2. The channels from Flow 2 have created a streamlined 'island', but measurements and observations show that prior to Flow 2, this area was two or more smaller 'islands' that the channels from Flow 1 had formed.

Figure 6: Maps and topographic profiles of Location 3 centred at 15.58° N, 162.37° E showing details of channels and cross-cutting relationships (see Figure 2 for location). (a) Map 1 – CTX mosaic with MOLA transects. (b) Map 2 – CTX with MOLA transects (black lines a'- a through d'- d) and interpreted channel markings/flow directions/ recessional terrace markings. (c) Inset located in (a) from CTX data showing details of a channel floor and margin. We interpret the presence of longitudinal lineations and recessional terraces (see caption to Figure 4). Talus slopes cover the channel margin in the NE. We have not identified features that would indicate lava flows such as lobate flow fronts or rootless cones. (d) Topographic profiles a'- a through d'- d. for each of the four transects with the blue line in each profile representing the MOLA transects. The vertical exaggeration for each topographic profile is x70. Overall our interpretation for Location 3 is that a broad Flow 1 channel oriented to the east or NE was cross-cut by a later flow (Flow 2) that cut a channel indicating flow towards the SE.

Figure 7: Maps and topographic profiles of Location 4 centred at 15.60° N, 162.75° E showing details of channels and cross-cutting relationships (see Figure 2 for location).

(a) Map 1 – CTX mosaic with MOLA transects. (b) Map 2 – CTX with MOLA transects (black lines a’- a through e’- e) and illustrated channel markings/flow directions/ recessional terrace markings. (c) Inset located in (a) from CTX data showing details of a channel floor and margin. We interpret the presence of longitudinal lineations and recessional terraces (see caption to Figure 4). We have not identified features that would indicate lava flows such as lobate flow fronts or rootless cones. (d) Topographic profiles a’- a through e’- e for each of the five transects with the blue line in each profile representing the MOLA transects. The vertical exaggeration for each topographic profile is x80. Our overall interpretation of Location 4 is that a Flow 3 channel cross-cuts and incises into a channel from Flow 1. The age of the Flow 1 channel is interpreted from the observation that it can be mapped back to its source (see Figures 2 and 3). The Flow 3 channel indicates flow towards the NE. As seen from topographic profiles c’- c, d’- d and e’- e the base of the Flow 3 channel is at approximately -2325 metres elevation at its deepest. This location appears to cross-cut a Flow 1 channel, possibly a remnant channel of Flow 1 that has not been covered by Flow 2 channels. The fissures are younger geological features, with recessional terrace markings from the flows disrupted by them.

Figure 8: Maps and topographic profiles of Location 5 centred at 15.13° N, 163.21° E showing details of channels and cross-cutting relationships (see Figure 2 for location). (a) Map 1 – CTX mosaic with MOLA transects. (b) Map 2 – CTX with MOLA transects (black lines a’- a through e’- e) and interpreted channel markings/flow directions/ recessional terrace markings. An area containing possible rootless cones is adjacent to a later fissure system, and we interpret the cones to related to volcanism associated with the fissures that post-dates channel formation. (c) Inset showing details of channel floor from HiRISE image ESP_025789_1950. No rootless cones are seen over most of the channel, for example as shown herein. (d) Topographic profiles a’- a through e’- e for each of the five transects with the blue line in each profile representing the MOLA transects. Location 5 maps (centred at) and topographic profiles show an area of possibly three flow channels. The vertical exaggeration for each topographic profile is x80. Our overall interpretation of Location 5 is that a channel from Flow 4 cross-cuts and incises into older channels.

Figure 9: Maps and topographic profiles of Location 6 centred at 15.60° N, 163.30° E showing details of channels and cross-cutting relationships (see Figure 2 for location). (a) Map 1 – CTX mosaic with MOLA transects. (b) Map 2 – CTX with MOLA transects (black lines a'- a through e'- e) and illustrated channel markings/flow directions/ recessional terrace markings. Fissure extension took place after the flow episodes, with the new fissures formations running parallel with the major fissure running through this region, approximately 16 km to the south-west of the newly formed fissure. (c) Inset from HiRISE image ESP_028756_1960 showing details of a channel floor and margins. We interpret the presence of longitudinal lineations and recessional terraces (see caption to Figure 4). We have not identified features that would indicate lava flows such as lobate flow fronts or rootless cones. (d) Topographic profiles a'- a through e'- e for each of the five transects with the blue line in each profile representing the MOLA transects. The vertical exaggeration for each topographic profile is x35. Our overall interpretation of Location 6 is that Flow 4 channels cross-cut earlier Flow 3 channels. There also exist remnant recessional terraces from a possible Flow 2 channel.

Figure 10: Maps and topographic profiles of Location 7 centred at 15.46° N, 163.28° E showing details of channels and cross-cutting relationships (see Figure 2 for location). (a) Map 1 – CTX mosaic with MOLA transects. (b) Map 2 – CTX with MOLA transects (black lines a'- a through e'- e) and illustrated channel markings/flow directions/ recessional terrace markings. (c) Inset from HiRISE image ESP_028400_1955 showing details of a channel floor and margins. We interpret the presence of longitudinal lineations and recessional terraces (see caption to Figure 4). We have not identified features that would indicate lava flows such as lobate flow fronts or rootless cones. (d) Topographic profiles a'- a through e'- e for each of the five transects with the blue line in each profile representing the MOLA transects. The vertical exaggeration for each topographic profile is x110. Our overall interpretation of Location 7 is that channels from Flow 4 flowed to the east, cross-cutting earlier flow channels formed by Flow 3 channels.

Figure 11: Shows the base elevations of identified flow channels in Locations 1 through 7, marked on the topographic profiles as L1, L2, L3, etc. The lowest elevation for each channel was used for each location and the estimated elevation at source for each flow episode (Flows 1 through 5). The last three points on Flow 3 are very close

together (within ~10-20 km) and within <10 m of each other vertically, and the same is true for the last three points in Flow 4; this is less than the uncertainty on vertical measurements from MOLA (±10 m). We consider them to be at the same height within error and the likely slight downward slope cannot be measured, but also cannot be excluded within error. The vertical exaggeration for the topographic profile is x80.

Figure 12: Schematic summary of cross-cutting relationships between channels. Time 1 took place before the later Time 2. In Time 1, a flow occurred at S1, and the flow formed distributary channels (Dc) that can all be mapped back to the source of the flow, S1. In Time 2, a later flow S2 occurred further east than the earlier S1. The flow from S2 formed distributary channels which cross cut the earlier distributary channels formed by S1 flows. In Time 2, we now see that only three of the five S1 distributary channels can be mapped back to their S1 source. This is why it is challenging to map some distributary channels back to the source of the flows. Speculative dike geometry at depth.

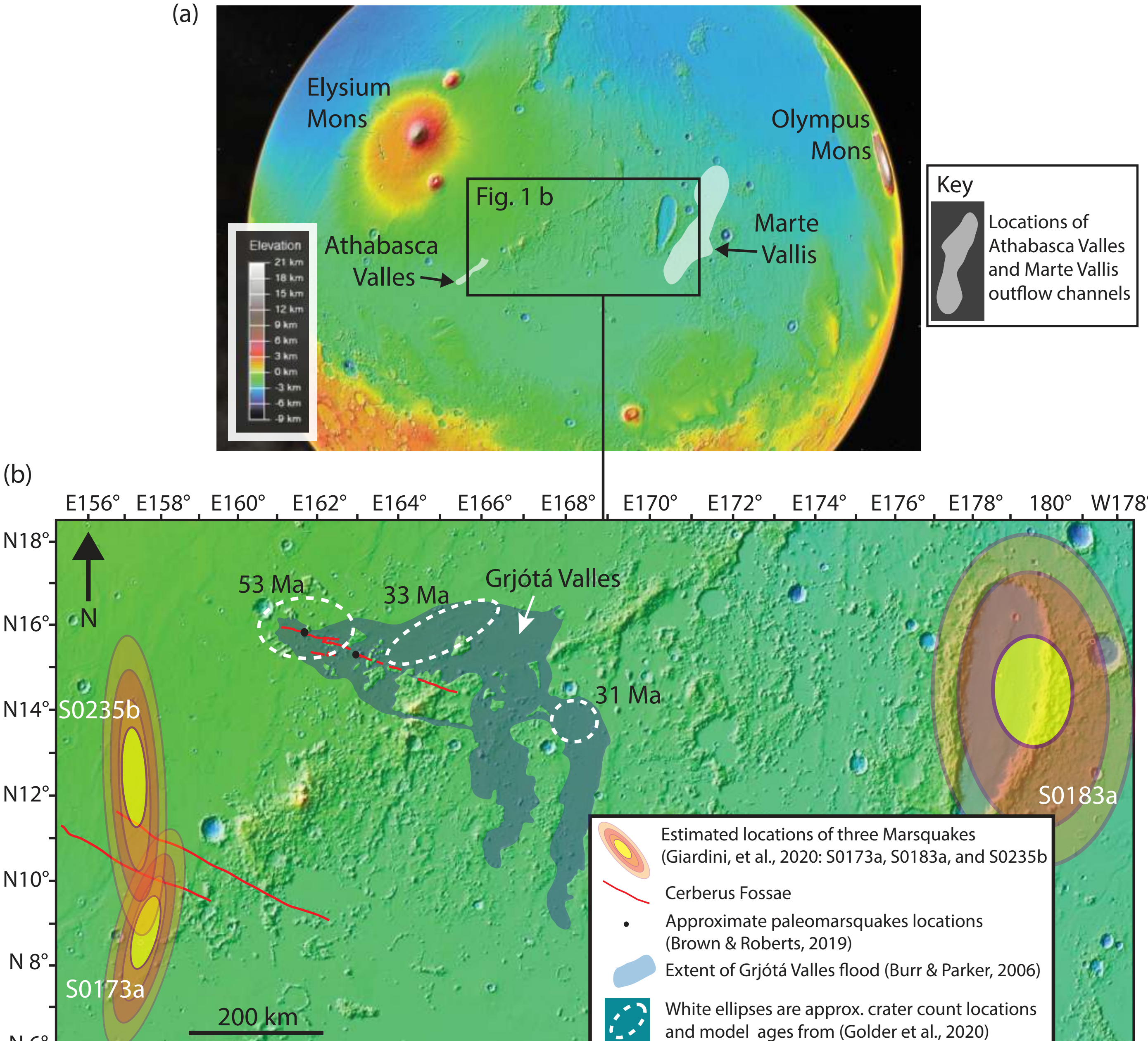

(a)
Elysium Mons
Olympus Mons
Fig. 1 b
Athabasca Valles
Marte Vallis
Elevation
21 km
18 km
15 km
12 km
9 km
6 km
3 km
0 km
-3 km
-6 km
-9 km
Key
Locations of Athabasca Valles and Marte Vallis outflow channels
(b)
E156° E158° E160° E162° E164° E166° E168° E170° E172° E174° E176° E178° 180° W178°
N18° N16° N14° N12° N10° N 8° N 6°
N
53 Ma
33 Ma
Grjótá Valles
31 Ma
S0235b
S0173a
S0183a
200 km
Estimated locations of three Marsquakes (Giardini, et al., 2020: S0173a, S0183a, and S0235b
Cerberus Fossae
Approximate paleomarsquakes locations (Brown & Roberts, 2019)
Extent of Grjótá Valles flood (Burr & Parker, 2006)
White ellipses are approx. crater count locations and model ages from (Golder et al., 2020)

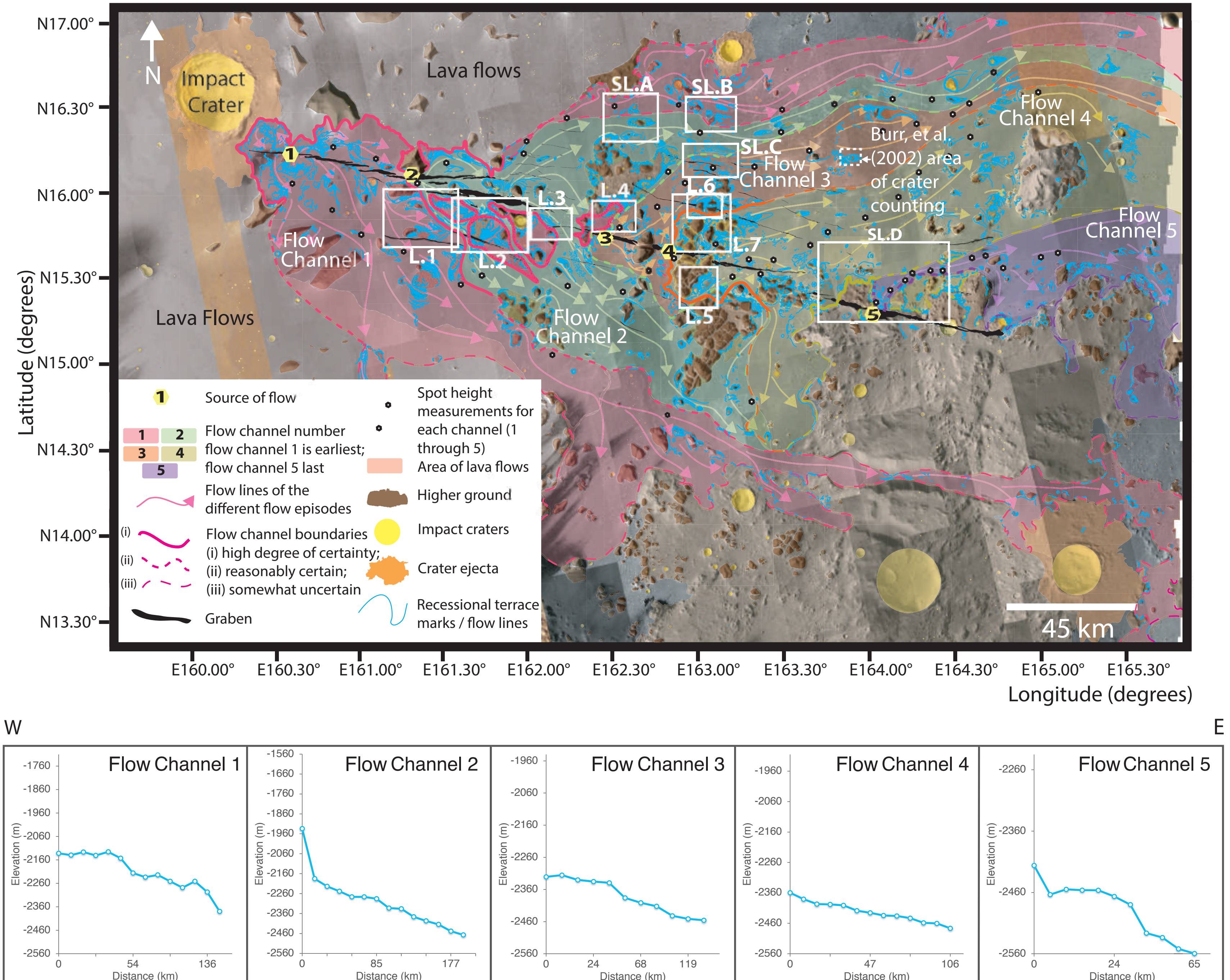

N17.00°
N16.30°
N16.00°
N15.30°
N15.00°
N14.30°
N14.00°
N13.30°
Latitude (degrees)
N
Impact Crater
Lava flows
Lava Flows
SL.A
SL.B
SL.C
SL.D
L.1
L.2
L.3
L.4
L.5
L.6
L.7
Flow Channel 1
Flow Channel 2
Flow Channel 3
Flow Channel 4
Flow Channel 5
Burr, et al, (2002) area of crater counting
Source of flow
Flow channel number flow channel 1 is earliest; flow channel 5 last
Flow lines of the different flow episodes
Flow channel boundaries (i) high degree of certainty; (ii) reasonably certain; (iii) somewhat uncertain
Graben
Spot height measurements for each channel (1 through 5)
Area of lava flows
Higher ground
Impact craters
Crater ejecta
Recessional terrace marks / flow lines
45 km
E160.00°
E160.30°
E161.00°
E161.30°
E162.00°
E162.30°
E163.00°
E163.30°
E164.00°
E164.30°
E165.00°
E165.30°
Longitude (degrees)
W
E
Flow Channel 1
Flow Channel 2
Flow Channel 3
Flow Channel 4
Flow Channel 5
Elevation (m)
Distance (km)

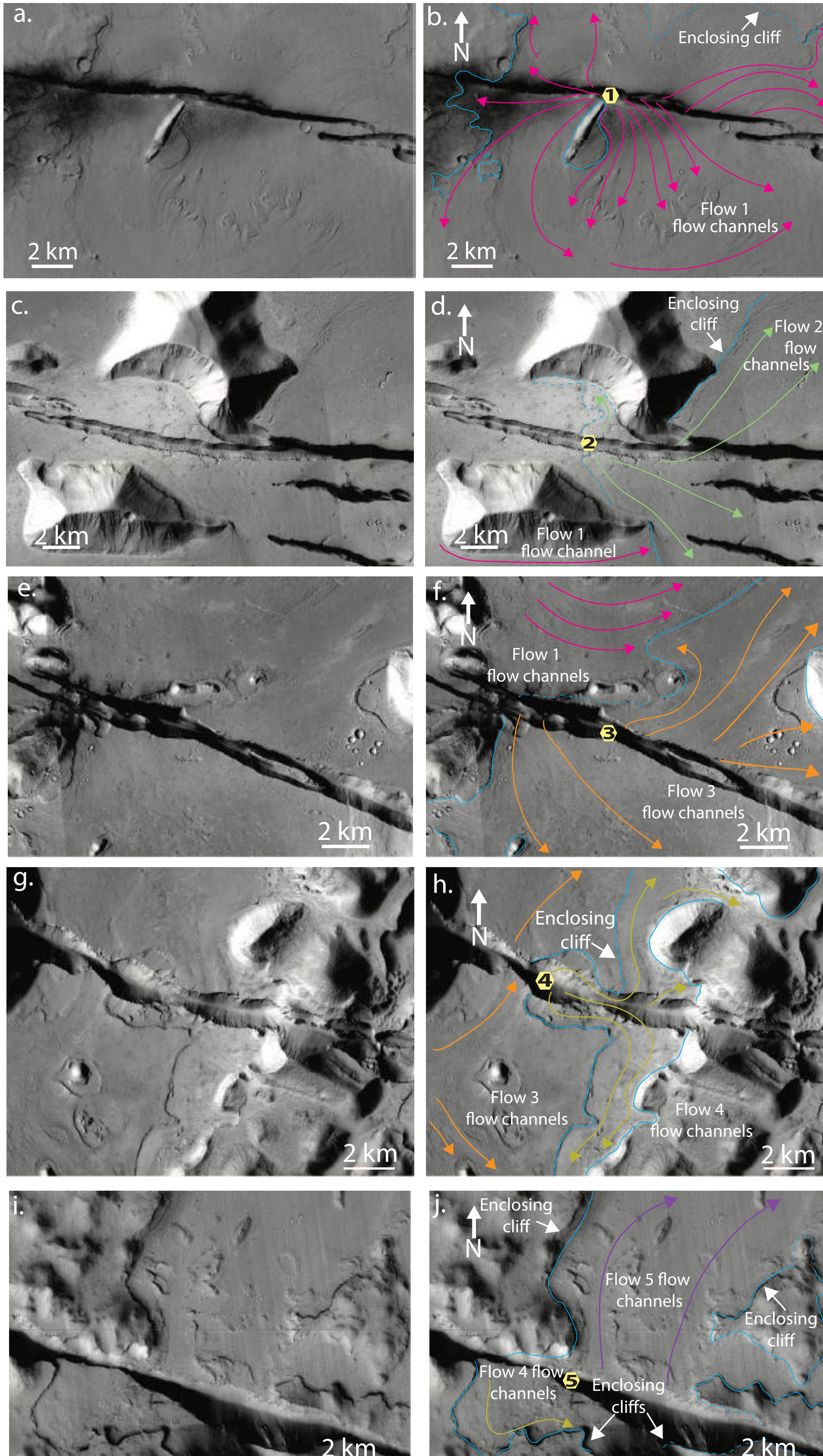
a.
2 km
b.
N
Enclosing cliff
1
Flow 1
flow channels
2 km
c.
2 km
d.
N
Enclosing
cliff
Flow 2
flow
channels
2
2 km
Flow 1
flow channel
e.
2 km
f.
N
Flow 1
flow channels
3
Flow 3
flow channels
2 km
g.
2 km
h.
N
Enclosing
cliff
4
Flow 3
flow channels
Flow 4
flow channels
2 km
i.
2 km
j.
Enclosing
cliff
N
Flow 5 flow
channels
Enclosing
cliff
Flow 4 flow
channels
5
Enclosing
cliffs
2 km

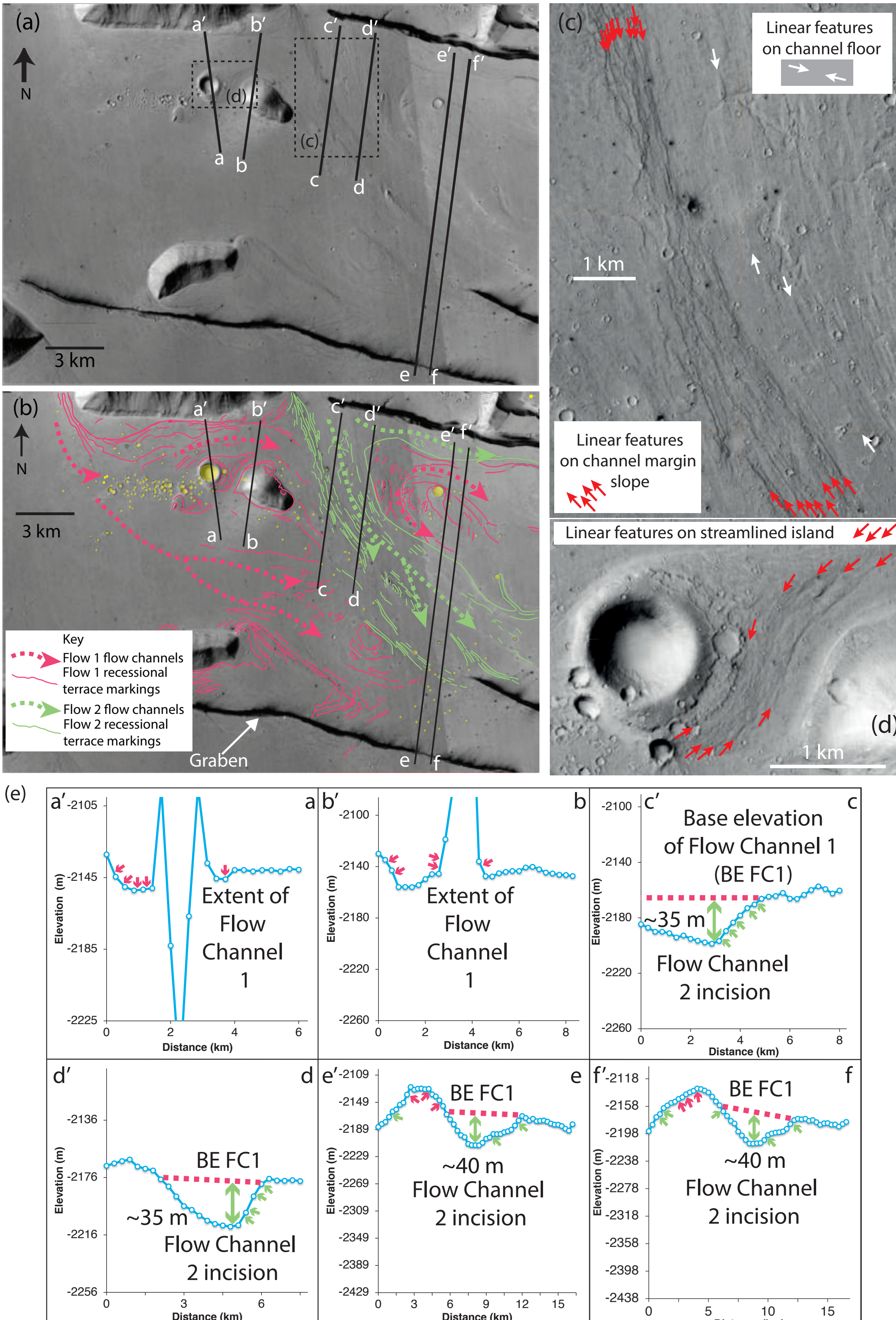
(a)
a′ b′ c′ d′ e′ f′
a b c d e f
(d)
(c)
N
3 km
(b)
Key
Flow 1 flow channels
Flow 1 recessional terrace markings
Flow 2 flow channels
Flow 2 recessional terrace markings
Graben
(c)
Linear features on channel floor
1 km
Linear features on channel margin slope
Linear features on streamlined island
(d)
1 km
(e)
Extent of Flow Channel 1
Base elevation of Flow Channel 1 (BE FC1)
~35 m
Flow Channel 2 incision
BE FC1
~40 m
Elevation (m)
Distance (km)

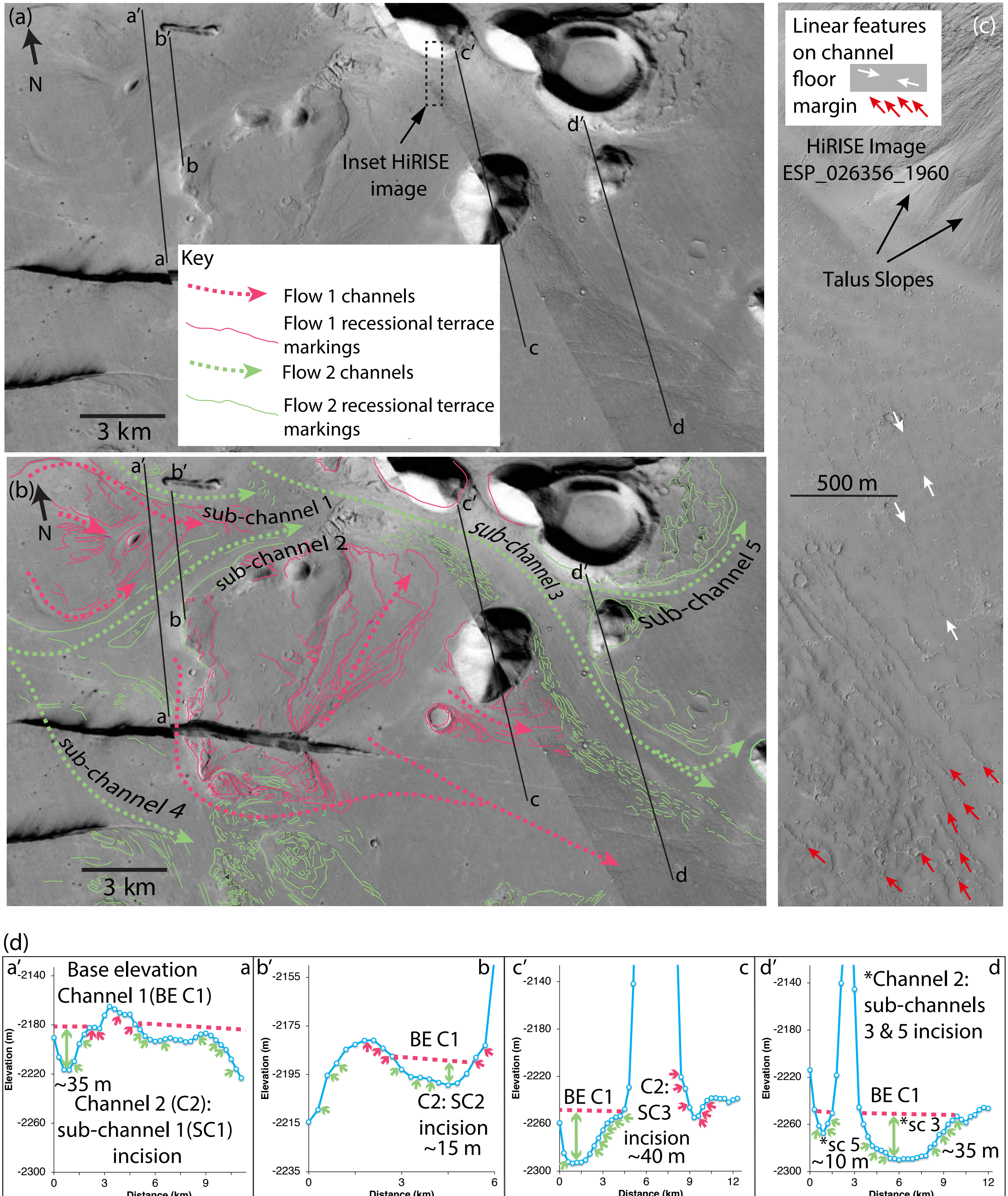

(a)
N
a′
b′
c′
d′
a
b
c
d
Inset HiRISE image
3 km
Key
Flow 1 channels
Flow 1 recessional terrace markings
Flow 2 channels
Flow 2 recessional terrace markings
(b)
sub-channel 1
sub-channel 2
sub-channel 3
sub-channel 4
sub-channel 5
(c)
Linear features on channel
floor
margin
HiRISE Image ESP_026356_1960
Talus Slopes
500 m
(d)
Base elevation Channel 1(BE C1)
~35 m
Channel 2 (C2): sub-channel 1(SC1) incision
BE C1
C2: SC2 incision ~15 m
C2: SC3 incision ~40 m
*Channel 2: sub-channels 3 & 5 incision
*sc 5 ~10 m
*sc 3
~35 m
Elevation (m)
Distance (km)

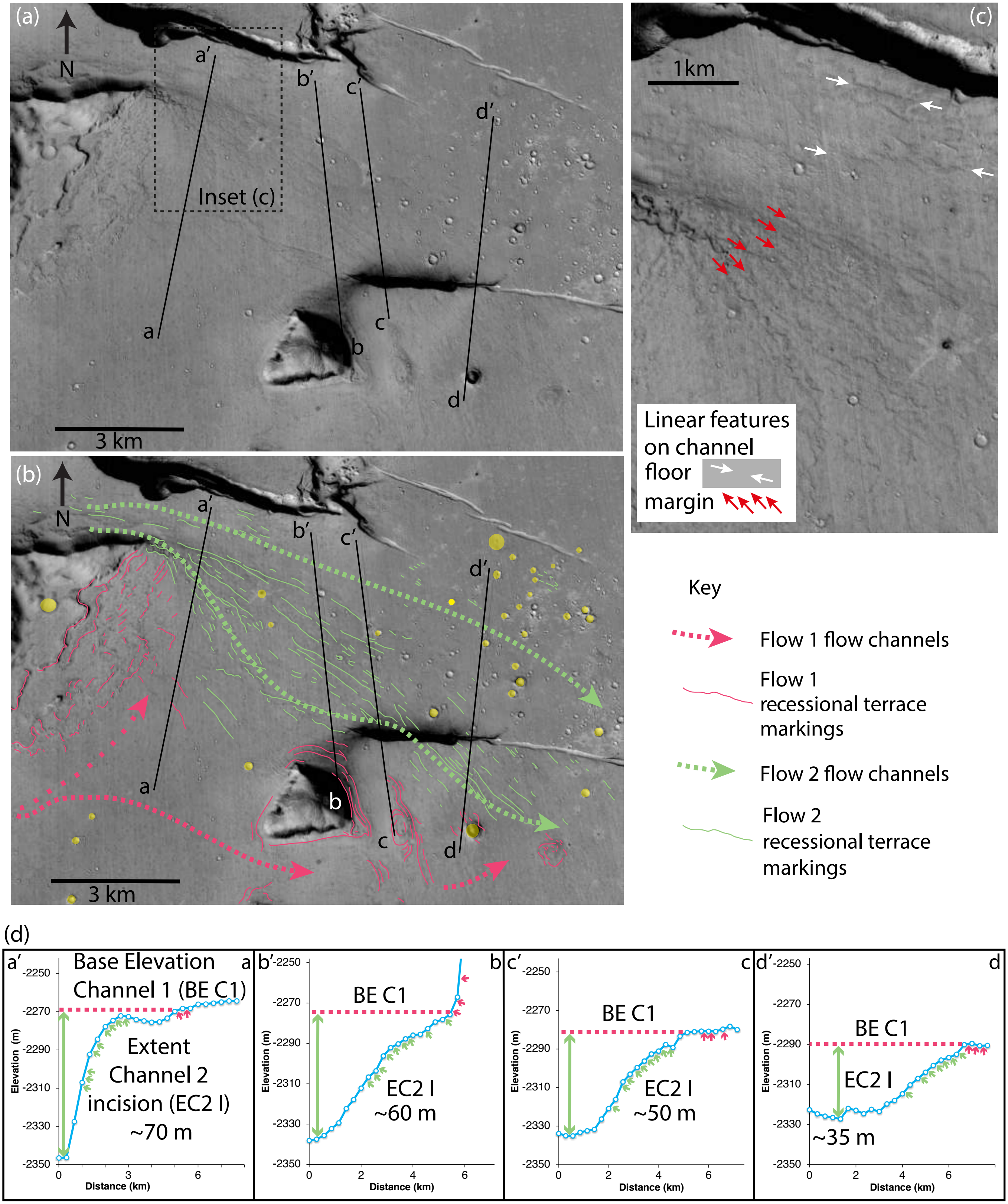
(a)
N
a′
b′
c′
d′
Inset (c)
a
b
c
d
3 km
(b)
(c)
1km
Linear features on channel
floor
margin
Key
Flow 1 flow channels
Flow 1 recessional terrace markings
Flow 2 flow channels
Flow 2 recessional terrace markings
(d)
Base Elevation Channel 1 (BE C1)
Extent Channel 2 incision (EC2 I) ~70 m
BE C1
EC2 I ~60 m
EC2 I ~50 m
EC2 I
~35 m
Elevation (m)
Distance (km)

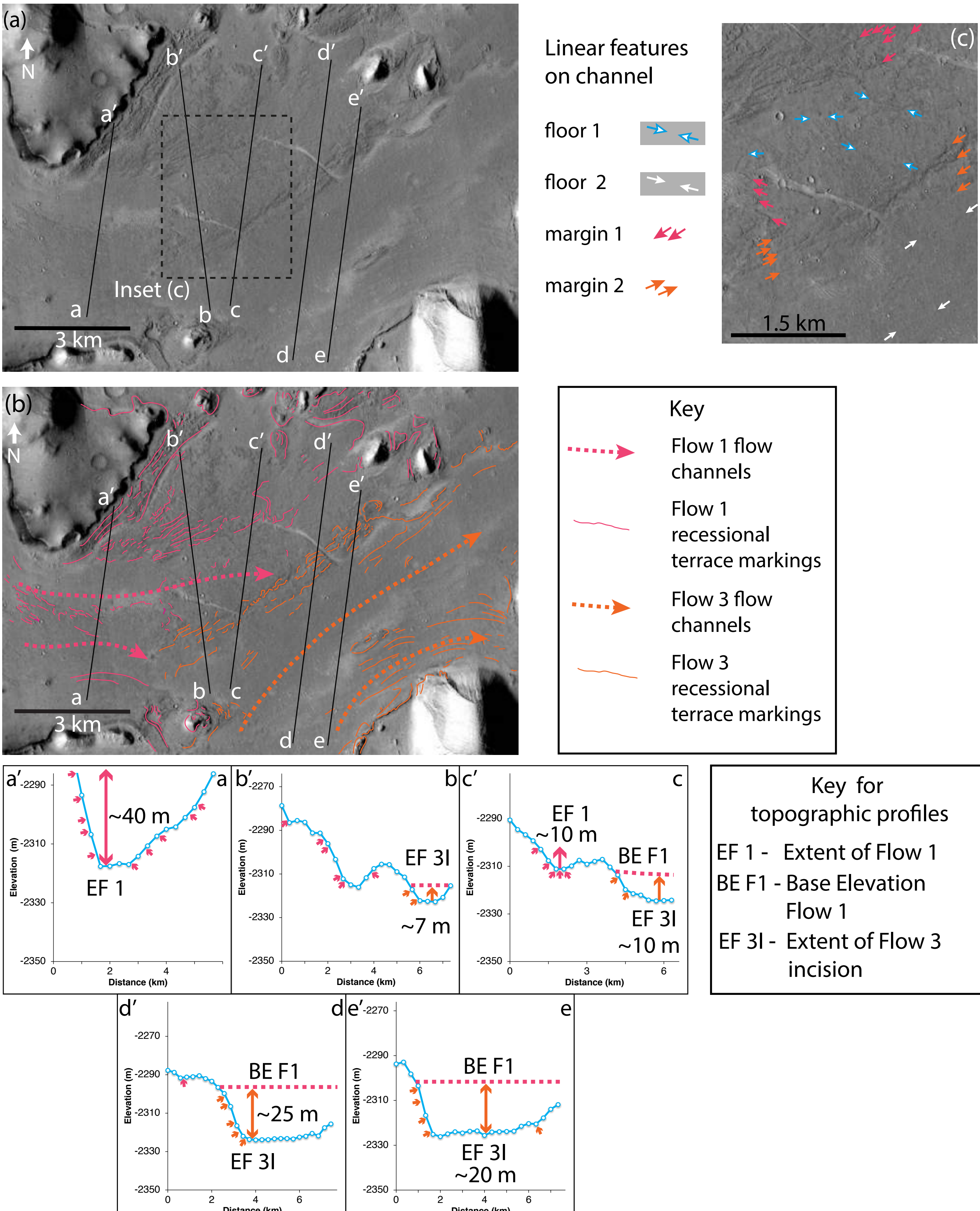

(a)
N
a′
b′
c′
d′
e′
Inset (c)
a
b
c
d
e
3 km
Linear features on channel
floor 1
floor 2
margin 1
margin 2
(c)
1.5 km
(b)
N
a′
b′
c′
d′
e′
a
b
c
d
e
3 km
Key
Flow 1 flow channels
Flow 1 recessional terrace markings
Flow 3 flow channels
Flow 3 recessional terrace markings
a′
a
~40 m
EF 1
Elevation (m)
Distance (km)
b′
b
EF 3I
~7 m
c′
c
EF 1
~10 m
BE F1
EF 3I
~10 m
Key for topographic profiles
EF 1 - Extent of Flow 1
BE F1 - Base Elevation Flow 1
EF 3I - Extent of Flow 3 incision
d′
d
BE F1
~25 m
EF 3I
e′
e
BE F1
EF 3I
~20 m

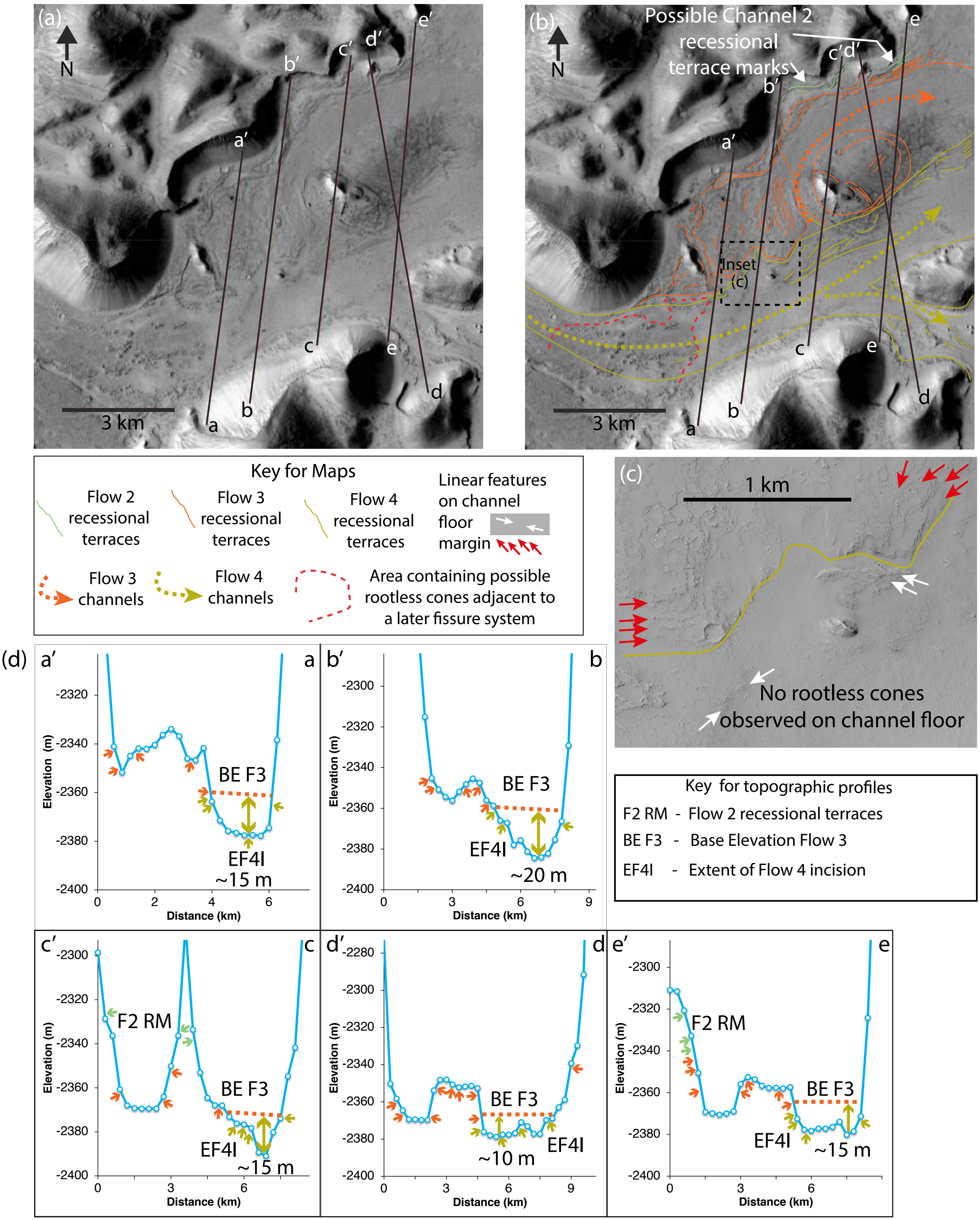

(a)
N
3 km
a a′ b b′ c c′ d d′ e e′
(b)
Possible Channel 2
recessional
terrace marks
Inset
(c)
3 km
(c)
1 km
No rootless cones
observed on channel floor
Key for Maps
Flow 2 recessional terraces
Flow 3 recessional terraces
Flow 4 recessional terraces
Linear features on channel floor margin
Flow 3 channels
Flow 4 channels
Area containing possible rootless cones adjacent to a later fissure system
Key for topographic profiles
F2 RM - Flow 2 recessional terraces
BE F3 - Base Elevation Flow 3
EF4I - Extent of Flow 4 incision
(d)
Elevation (m)
Distance (km)
BE F3
EF4I
~15 m
~20 m
F2 RM
~10 m

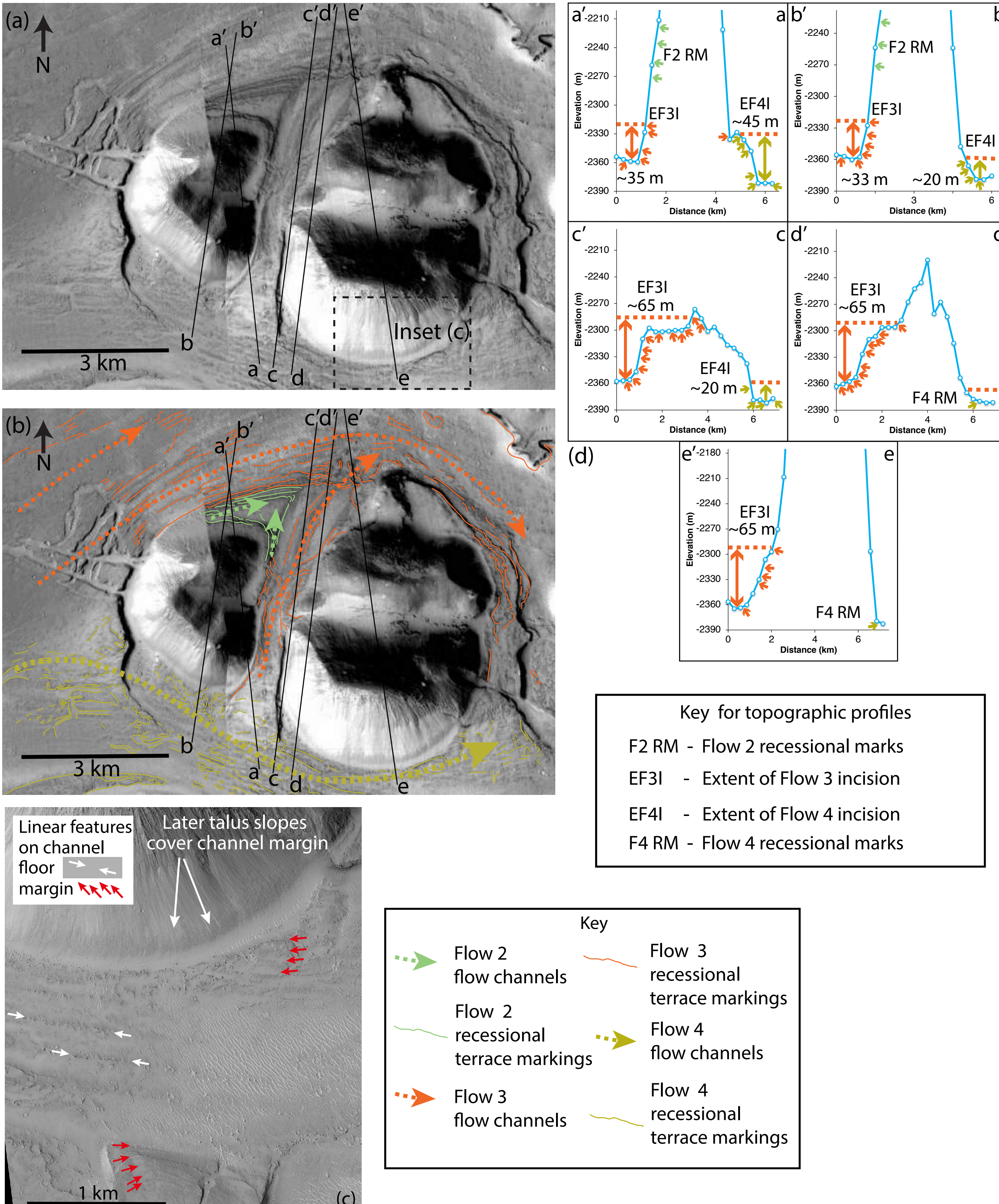

(a)
N
a′ b′
c′d′ e′
3 km
b
a c d
Inset (c)
e
(b)
N
a′ b′
c′d′ e′
3 km
b
a c d
e
Linear features on channel
floor
margin
Later talus slopes cover channel margin
1 km
(c)
a′ a
F2 RM
EF3I
EF4I
~45 m
~35 m
Elevation (m)
Distance (km)
b′ b
F2 RM
EF3I
EF4I
~33 m
~20 m
c′ c
EF3I
~65 m
EF4I
~20 m
d′ d
EF3I
~65 m
F4 RM
(d)
e′ e
EF3I
~65 m
F4 RM
Key for topographic profiles
F2 RM - Flow 2 recessional marks
EF3I - Extent of Flow 3 incision
EF4I - Extent of Flow 4 incision
F4 RM - Flow 4 recessional marks
Key
Flow 2 flow channels
Flow 2 recessional terrace markings
Flow 3 flow channels
Flow 3 recessional terrace markings
Flow 4 flow channels
Flow 4 recessional terrace markings

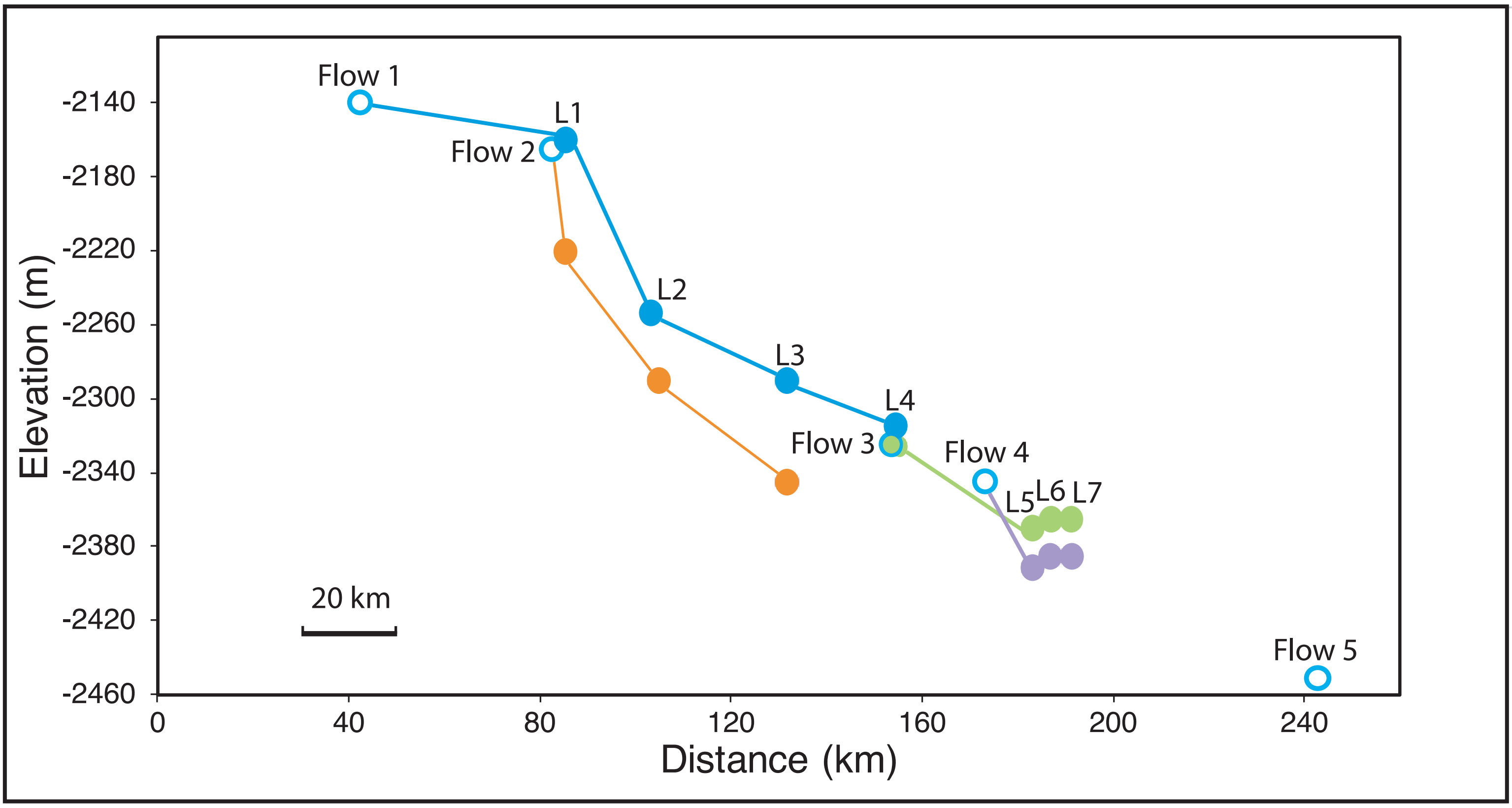

Channel 1 base elevation
Channel 2 base elevation
Channel 3 base elevation
Channel 4 base elevation

Estimated location of each flow (1 through 5) at source

L1 through L7 - Channel base elevations at each location

Supporting Information for

Repeated, cross-cutting and spatially migrating outflow channel formation, Grjótá Valles, Mars

Jason R. Brown, Gerald P. Roberts,
Department of Earth and Planetary Sciences, Birkbeck, University of London, WC1E 7HX, United Kingdom

Contents of this file

Text S1 to S4

Figures S1 to S4

Captions S1 to S4

Introduction

Supplementary locations S1 to S4 are provided as evidence of the lateral extent of the landforms produced by the flows in downstream locations. It was found that it is more challenging to define cross-cutting relationships with distance from the flow sources because the incision generally decreases downstream and channel courses tend to run almost parallel to each other in a west to east direction. Thus, it was necessary to focus on locations that did not necessarily exhibit clear cross-cutting relationships, but instead offered evidence through geological observation and/or analyses of MOLA data to possible positions of boundary lines between the different flow episodes.

The supplementary locations S1 to S4 helped us to construct Figure 2 within the main manuscript.

Figure S1: Map 1 – CTX with MOLA transects (black lines a'- a through e'- e) and illustrated channel markings/flow directions/recessional terrace markings; Topographic profiles a'- a through e'- e for each of the five transects with the blue line in each profile representing the MOLA transects. Supplementary location maps (centred at 16.15° N, 162.90° E) and topographic profiles show the possible flow boundary between the earlier Flow 1 channels and the younger Flow 2 channels. The position of observed recessional terrace marks, and to what flow they belong, are marked on the topographic profiles as arrows in colours corresponding to the flow colour. The vertical exaggeration for each topographic profile is x400.

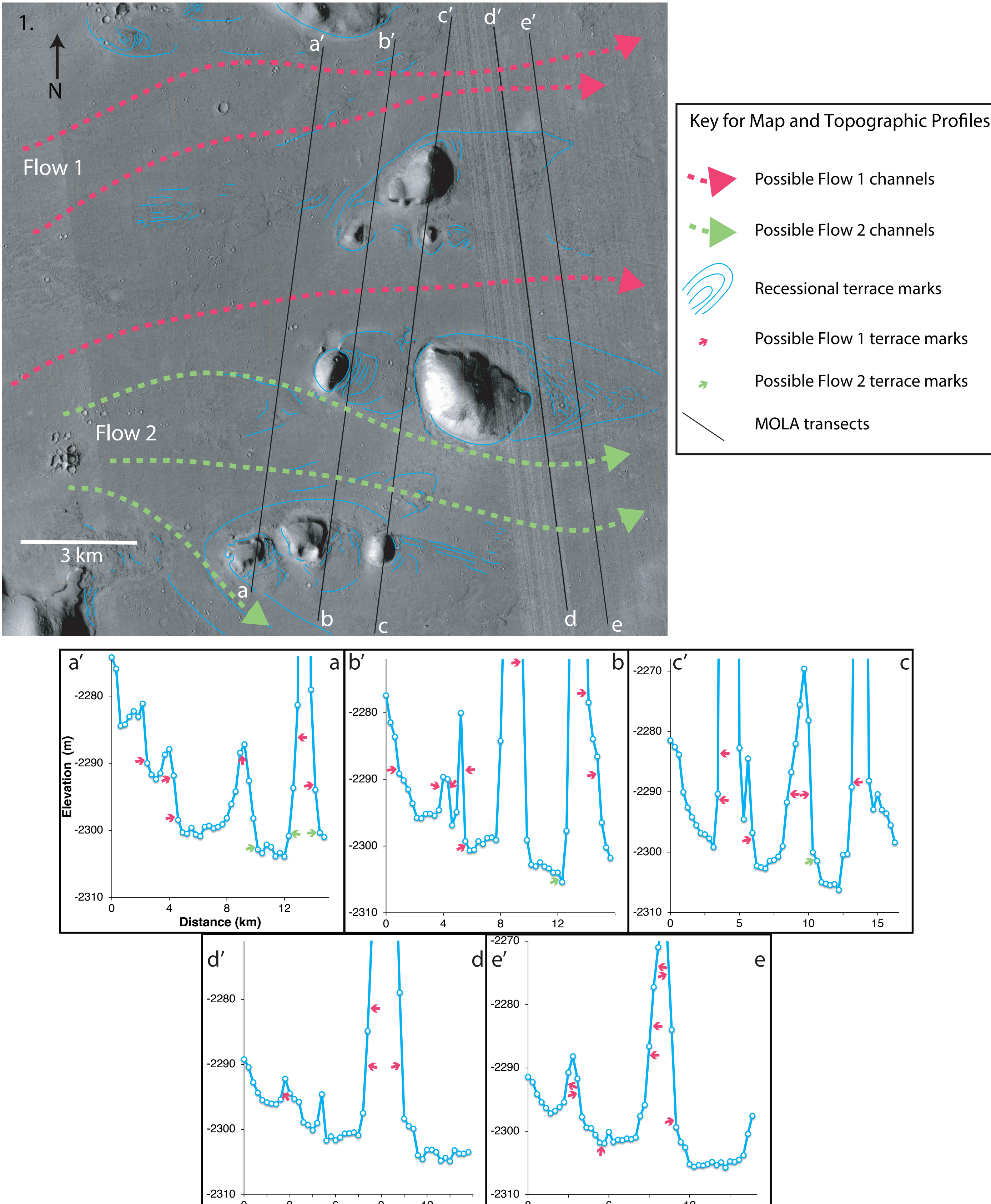
1.
N
Flow 1
Flow 2
3 km
a′
b′
c′
d′
e′
a
b
c
d
e
Key for Map and Topographic Profiles
Possible Flow 1 channels
Possible Flow 2 channels
Recessional terrace marks
Possible Flow 1 terrace marks
Possible Flow 2 terrace marks
MOLA transects
Elevation (m)
Distance (km)
-2270
-2280
-2290
-2300
-2310
0
3
4
5
6
8
9
10
12
15

Figure S2: Map 1 – CTX with MOLA transects (black lines a'- a through f'- f) and illustrated channel markings/flow directions/recessional terrace markings; Topographic profiles a'- a through f'- f for each of the six transects with the blue line in each profile representing the MOLA transects. Supplementary location map (centred at 16.13° N, 163.37° E) and topographic profiles shows the possible flow boundary between the earlier Flow 1 channels and the younger Flow 2 channels. A boundary between the two flows appears to be delineated by the area of higher ground. This is an area of higher ground that may well have served as a natural boundary between Flow 1 and Flow 2 channels. The position of observed recessional terrace marks, and to what flow they belong, are marked on the topographic profiles as arrows in colours corresponding to the flow colour. The vertical exaggeration for each topographic profile is x100.

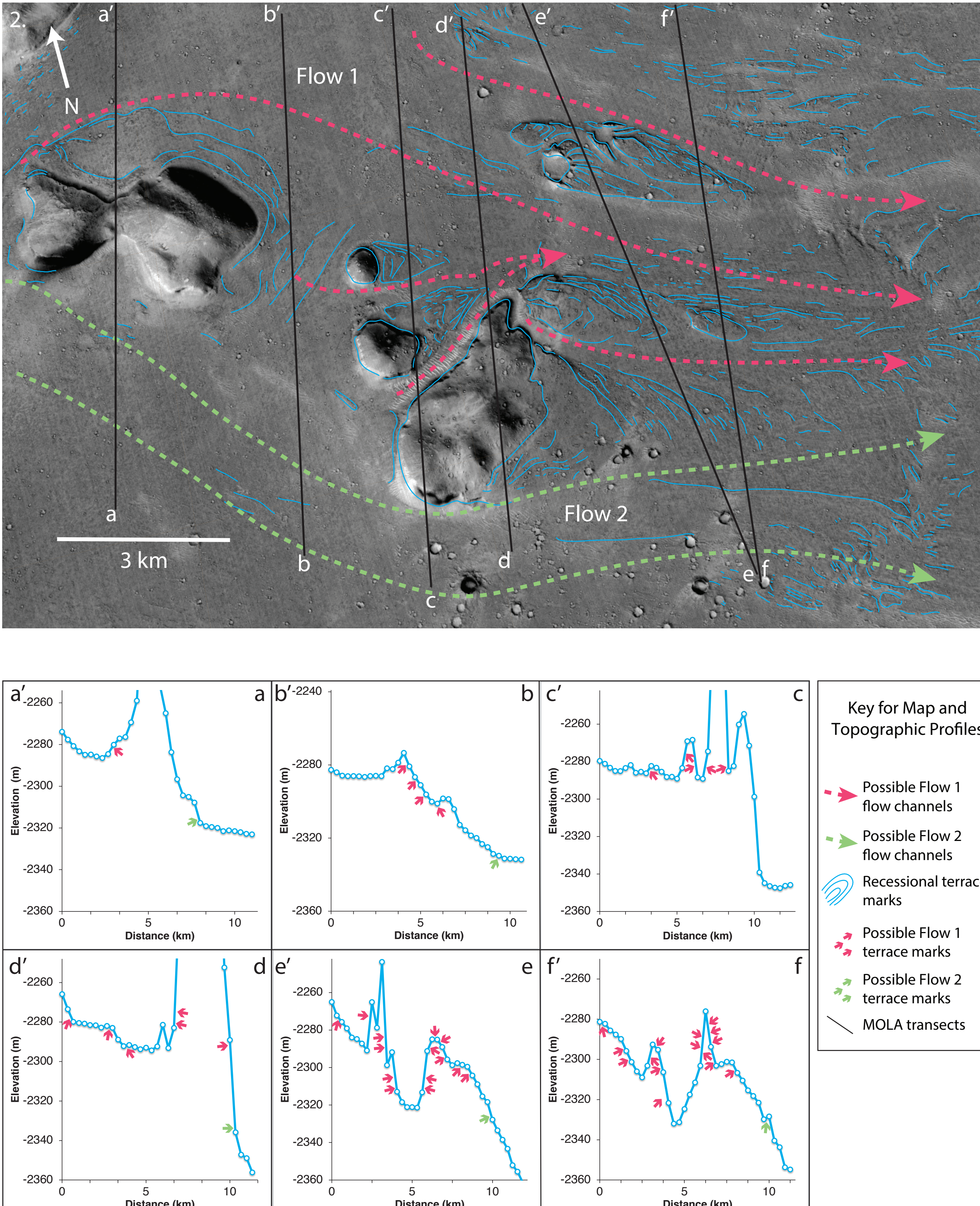
2.
N
a′
b′
c′
d′
e′
f′
Flow 1
Flow 2
a
b
c
d
e
f
3 km
Elevation (m)
Distance (km)
Key for Map and Topographic Profiles
Possible Flow 1 flow channels
Possible Flow 2 flow channels
Recessional terrace marks
Possible Flow 1 terrace marks
Possible Flow 2 terrace marks
MOLA transects

Figure S3: Map 1 – CTX with MOLA transects (black lines a'- a through e'- e) and illustrated channel markings/flow directions/recessional terrace markings; Topographic profiles a'- a through e'- e for each of the five transects with the blue line in each profile representing the MOLA transects. Supplementary Location C maps (centred at 15.83° N, 163.36° E) and topographic profiles. Show the boundary between Flow 2 and Flow 3. As the geomorphic features within Map 1 and Map 2 show, the orientation of the features shaped by Flow 2 suggests that flow movement appears to have moved from the north-west, and flowed south-east, before reaching a depression, after which the course of the flow is in an east by south direction. The orientation of the features shaped by Flow 3 suggests that flow movement appears to have moved from south-west, and flowed in a north-east / east direction.

Also, Supplementary Location maps A and B reveal the position of Flood 2 flow channels west of this location and both clearly show that Flow 2 channels were flowing in an easterly direction. The flow pattern for Flow 3 channels in Map 2 above ties in with the flow boundaries for Flows 2 and 3 in the Location 4 maps and topographic profiles. Map 2 shows the estimated Flow 3 boundary. The position of observed recessional terrace marks, and to what flow they belong, are marked on the topographic profiles as arrows in colours corresponding to the flow colour. Fissure formations, that run parallel with the major fissure formation 34 km to the south, are young formations, certainly younger than the flow episodes, clearly displacing Flow 3 flow lines. The vertical exaggeration for each topographic profile is x150.

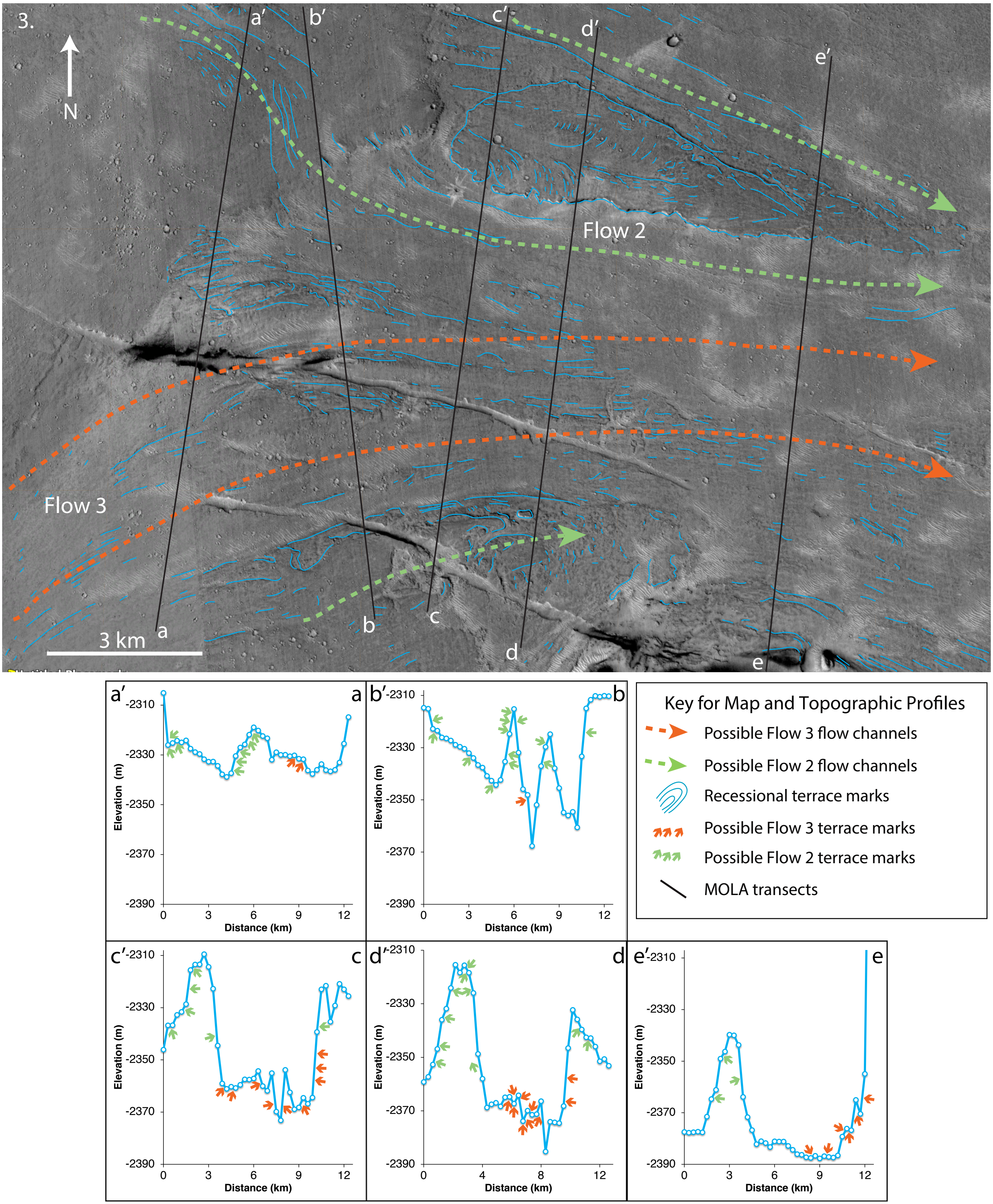

3.
N
a′
b′
c′
d′
e′
Flow 2
Flow 3
3 km
a
b
c
d
e
Elevation (m)
Distance (km)
-2310
-2330
-2350
-2370
-2390
Key for Map and Topographic Profiles
Possible Flow 3 flow channels
Possible Flow 2 flow channels
Recessional terrace marks
Possible Flow 3 terrace marks
Possible Flow 2 terrace marks
MOLA transects

Figure S4: Map 1 – CTX with MOLA transects (black lines a'- a through f'- f) and illustrated channel markings/flow directions/recessional terrace markings; Topographic profiles a'- a through f'- f for each of the six transects with the blue line in each profile representing the MOLA transects. Supplementary Location D maps (centred at 15.00° N, 164.35° E) and topographic profiles. Shows the boundaries between Flow 4 and Flow 5. The estimated emanation point for Flow 5 is marked on the lower section of Map 1 as the number 5 in a yellow hexagon. The authors estimate the source as here based in part on the MOLA data visible in topographic profiles a'- a through f'- f. Profile a'- a clearly shows unidirectional flow from west to east at an elevation that is in keeping with Flow 4 elevations further west, taking into consideration the sloping west to east topography. Profile b'- b follows a similar pattern until reaching an area close to the main fissure formation, where the elevation decreases and visible flow lines / recessional terrace marks are observed. The orientation of the streamlined bodies in this area strongly suggests a flow channel emanated from this area and flowed north-east. The fissure formation at the base of Map 1 is a younger formation than the flow channels and has clearly offset the recessional terrace markings of Flow 5 close to the source of Flow 5. The position of observed recessional terrace marks, and to what flow they belong, are marked on the topographic profiles as arrows in colours corresponding to the flow colour. The vertical exaggeration for each topographic profile is x150.

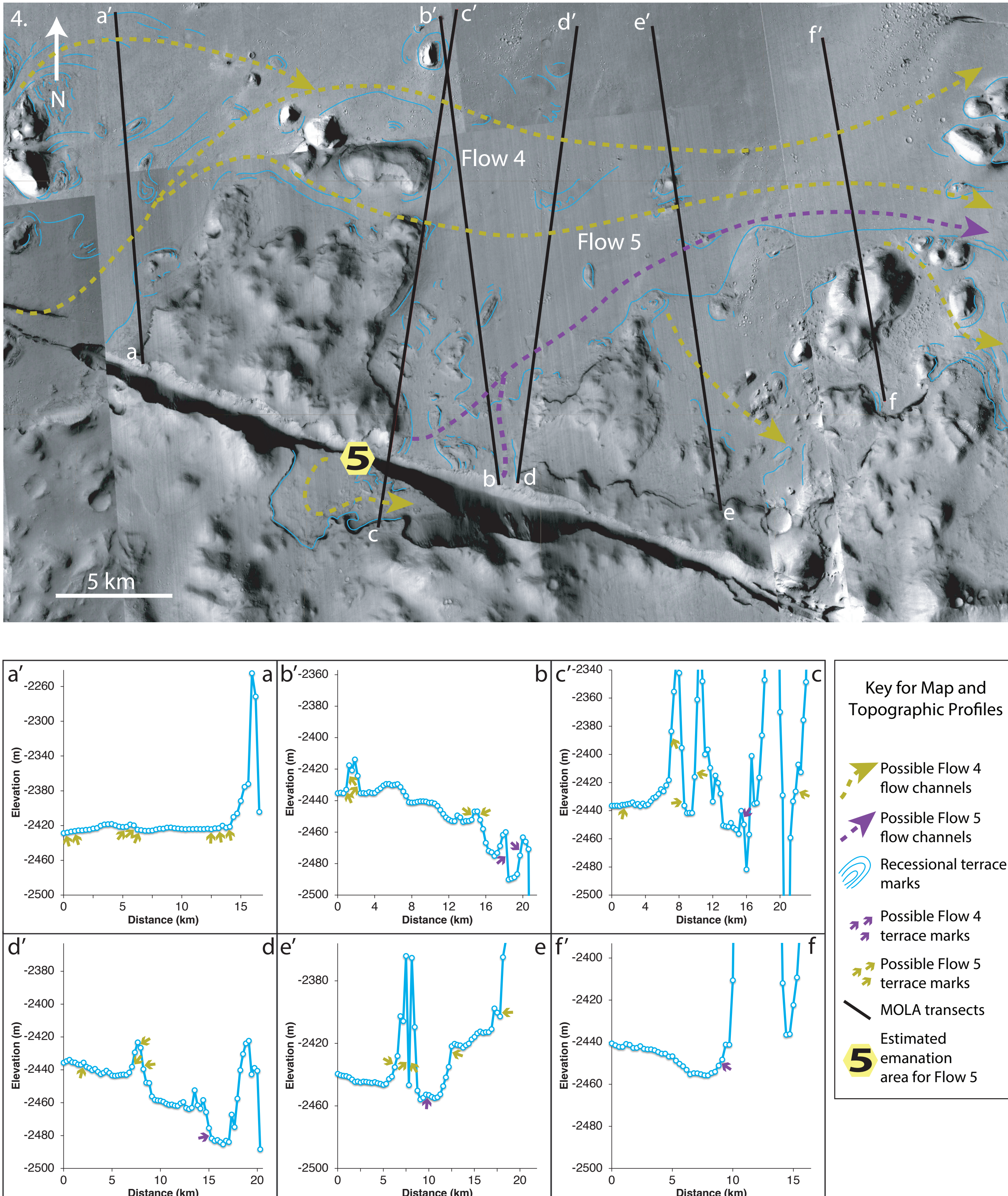
4.
N
a′
b′
c′
d′
e′
f′
a
b
c
d
e
f
Flow 4
Flow 5
5
5 km
Elevation (m)
Distance (km)
Key for Map and Topographic Profiles
Possible Flow 4 flow channels
Possible Flow 5 flow channels
Recessional terrace marks
Possible Flow 4 terrace marks
Possible Flow 5 terrace marks
MOLA transects
Estimated emanation area for Flow 5